NASA Contractor Report 178284

AEROELASTICITY AND MECHANICAL STABILITY REPORT,
0.27 MACH SCALE MODEL OF THE YAH-64 ADVANCED
ATTACK HELICOPTER

F. K. Straub and R. A. Johnston

MCDONNELL DOUGLAS HELICOPTER COMPANY
Mesa, Arizona

NASA

National Aeronautics and
Space Administration

Langley Research Center
Hampton, Virginia 23665

CONTENTS

SUMMARY

Hughes Helicopters, Inc., has provided NASA Langley Research Center a 0.27 Mach scaled model of the AH-64 Advanced Attack Helicopter main rotor and hub under Contract No. NAS1-16475. The model will be tested in NASA's V/STOL wind tunnel using the General Rotor Model System (GRMS).

This report documents the studies performed to ensure dynamic similarity of the model with its full scale parent. It also contains a preliminary aeroelastic and aeromechanical substantiation for the rotor installation in the wind tunnel. From the limited studies performed no aeroelastic stability or load problems are projected. To alleviate a projected ground resonance problem, a modification of the roll characteristics of the GRMS is recommended.

All results in this report are based on the ideally scaled blade properties. Actual model blade data were not available at the time. Appendix II contains a brief evaluation of the dynamic properties of an advanced blade for the AH-64 model rotor. This blade is developed by NASA under a separate contract.

At this time, the aeroelastic behavior of the coupled rotor/GRMS has not been fully explored. Loads and wind tunnel operational spectra have not been defined in sufficient detail. Also, a practical solution to the projected ground resonance problem must be quantified.

To ensure safe integration of the model rotor with the GRMS and to verify this through tests, HHI has defined follow-on studies in proposals No. 4513-7 and 4513-8.

PRECEDING PAGE BLANK NOT FiLMED

INTRODUCTION

Hughes Helicopters, Inc. (HHI) has designed, fabricated, and provided to NASA Langley Research Center a 0.27 Mach scaled model of the AH-64 Advanced Attack Helicopter (AAH) main rotor and hub under Contract No. NAS1-16475. An exploded view of the model rotor hub is shown in Figure I-1.

NASA proposes to use the rotor to conduct research in its V/STOL wind tunnel. For this purpose, the rotor will be mounted on NASA's General Rotor Model System (GRMS), Reference 1, the principal features of which are shown in Figure I-2. This system provides rotor control capability and also contains a balance to measure rotor loads. A capability is also provided to tune the fundamental roll and pitch modes through changes in the respective spring rates and damping. The GRMS and the sting to which it is attached form essentially a fixed structure to which test rotors must be integrated.

The full scale AAH main rotor has been tested extensively and has been demonstrated to have excellent dynamic characteristics. HHI has conducted a number of studies to guide the design of the model rotor. These studies have resulted in a model rotor that has dynamic characteristics that closely match that of the full scale rotor. There are, nevertheless, a number of important issues that have to be addressed. No attempt has been made to scale the dynamic properties of the GRMS to those of the AAH airframe and drive system. For this reason, scaled behavior of the coupled rotor/fuselage is essentially lost when the model rotor is mounted on the GRMS.

Integrating any rotor with any fixed structure always produces the possibility of adverse coupling among the two that can lead to aeromechanical or aeroelastic problems or excessive forced responses. This is particularly true for ground resonance since it is not possible to "fly out" of a problem as is generally the case with an actual rotorcraft. To address these issues

HHI has conducted preliminary analytical studies to define the dynamic characteristics, and project stability margins for the 0.27 scaled model AAH main rotor mounted on the GRMS. The analyses used are described in Reference 2 and 3. The DART analysis program (reference 2) was used for the dynamic, aeroelastic stability and loads studies, while the E-927 program (reference 3) was used for ground resonance only.

This report provides the results of studies conducted up to this time. It does not constitute a complete aeroelastic and aeromechanical evaluation of the coupled rotor/GRMS system.

Furthermore, results in this report are of preliminary nature inasmuch as they are based on ideally scaled blade properties.

1.0 OBJECTIVES

The objectives of the analytical studies described in this report are to

- Demonstrate that the 0.27 Mach scaled AAH main rotor has essentially the same dynamic characteristics as the full scale rotor, and to

- Investigate the aeromechanical stability of the model rotor integrated with the General Rotor Model System (GRMS).

2.0 MODEL ROTOR PROPERTIES

The appropriate scale factors for Mach scaling in air are given in Table 2-1. Table 2-2 shows the Mach scaled rotor properties compared to those for the full scale AAH main rotor. Tables 2-3 and 2-4 compare ideally scaled hub and blade data with that of the actual model design. Distributed model blade data are provided in Appendix A.

Model blade lag damper properties are directly scaled from those of the full scale AAH main rotor through the relationship:

Model Damper = 0.27 x Full Scale Damper,

see Table 2-5. Figure 2-1 shows the effect of lead-lag amplitude on the lag damper characteristics. The circles in Figure 2-1 indicate the specified damper properties, whereas the vertical bars show the range of properties obtained through tests of all twelve dampers.

3.0 GRMS DYNAMIC PROPERTIES

To permit analysis of the fully coupled rotor/GRMS system, certain dynamic properties of the GRMS have to be known. Since these data were not available, HHI defined the requirements and participated in a shake test of the GRMS at the NASA Langley V/STOL facility. Complete details of this test are contained in Reference [4].

Briefly, the data that are required for the analysis are the frequencies, generalized masses, generalized dampings, and modal components of motion at the main rotor hub for all of the natural modes of the GRMS within a specified frequency range. For the analysis described in this report, these data were defined for modes in the frequency range 0-100 Hz. Table 3-1 provides the measured data in the format used in the analysis. These modal data do not include the effects of blade weight or inertias, nor have any corrections been made to account for the correct hub weight and hub weight location.

4.0 MODEL ROTOR DYNAMICS

A comparison between the modal frequencies for the isolated model and full scale AAH rotor is given in Figure 4-1. These data assume all hub impedances are infinite. Except for the torsion mode, it can be seen that the model blade modes closely match those of the full scale blade.

Without involving GRMS hardware, the only way to match torsional frequency was through changes in the model pitch link stiffness. Retaining the ideally scaled AAH pitch link stiffness would have resulted in a first torsion mode frequency at about 5.6/rev. The softest practical pitch link would have resulted in a torsional resonance at 5/rev. Because of this, it was decided to make the pitch link stiffness such that the torsional frequency was above, and well separated from, 5/rev. Since with this model blade torsional frequency, both the model and full scale frequencies are separated from 5/rev, above and below respectively, it is not expected that the forced torsional responses will be significantly different.

The model rotor is therefore substantially dynamically similar to the full scale AAH main rotor.

To achieve this dynamic similarity, several design iterations had to be performed. For Mach scaling, as can be seen from Table 2-1, stresses remain constant whereas mass is scaled by the cube of the scale factor. Consequently, considerable effort was spent in reducing the weight of the rotor hub and the flapping hardware without compromising the loads criteria. Figure 4-2 shows for two intermediate configurations that the heavier flapping hardware lowers the elastic mode frequencies. For the first chord bending mode, this effect is compensated by the increased strap stiffness.

5.0 COUPLED-MODEL ROTOR/GRMS VIBRATION AND LOADS

The data provided in Section 3.0 show that the frequencies of the principal modes of the GRMS are separated from integer multiples of the number of blades in the model rotor times the rotor speed within the normal operating rotor speed range. Similarly, the isolated blade frequency data provided in Section 4.0 show that the blade modal frequencies are separated from the harmonics of rotor speed.

Coupling the model rotor to the GRMS can influence the blade and GRMS modes and thereby affect rotor loads and system vibration. An assessment of these effects can be made by examining the modes for the fully coupled rotor/ GRMS system.

For the isolated model rotor blade, the frequencies of the cyclic blade modes are coincident with those of the collective or reactionless modes given in Figure 4-1. Coupling the rotor to the GRMS will have no influence on the reactionless modes, but may affect the frequencies of the collective and cyclic modes of the blades. Neglecting drive system torsional dynamics, the results of a fully coupled rotor/GRMS analysis showed that blade collective modes were unaffected and that the cyclic modes were only slightly influenced.

Figures 5-1 and 5-2 show the advancing and regressing cyclic modes. Since the DART analysis requires isotropic rotor support properties, the pitching motion of the GRMS (modes at 12, 16, and 33.1 Hz) and rolling motion of the GRMS (modes at 8.9, 16.4, and 57 Hz) were considered separately. Comparison with full scale AAH data shows that frequency matching is generally good except for the torsion mode, as noted in Section 4.0, and the chord bending mode. The reason for the lowered chord bending frequency is the high effective mass associated with the GRMS shaft bending modes. For this same reason, the heavier than ideally scaled hub of the 0.27 scale model does not appreciably

change frequency placement of the chord bending mode. Comparing Figures 5-1 and 5-2 with Figure 4-1 shows that the cyclic modes, with the exception of the chord bending mode, are only slightly influenced.

Because the coupling of the rotor to the GRMS has not substantially degraded the separation of the blade modal frequencies from the rotor harmonics, it can be concluded that the forced response characteristics of the blades will likewise be little affected.

Depending on their relative values, the weight and inertial properties of the rotating blades can influence the GRMS modes. High rotor to GRMS effective mass/inertia ratios generally lead to stronger coupling. This has implications for stability (in particular ground resonance discussed in Section 8.0) and forced response. The relationships among the uncoupled GRMS mode frequencies and those for the fully coupled rotor/GRMS system are shown in Table 5-1 for model rotor speeds of 80%, 100%, and 120% N_R. It can be seen that the fundamental GRMS modes are not appreciably changed through coupling with the rotor. Assuming this to be true also for the higher GRMS modes, amplification of rotor loads can be expected to be minimal and vibration low. Hub vibratory motions should likewise be low and have little influence on the blade response characteristics. Loads developed from an isolated blade analysis should therefore be sufficient for the purpose of design integration. This consideration neglects aerodynamic interference effects between the rotor and the GRMS.

6.0 AEROELASTIC STABILITY

Apart from ground resonance, which is descussed in Section 8.0, it was shown in Section 5.0 that the blade modal frequencies are little affected by the GRMS dynamics. This indicates that there is insignificant coupling between the rotor and the GRMS. The addition of aerodynamic forces to the blades will not substantially alter this coupling, but they will influence the behavior of the blades themselves. Because the rotor to GRMS coupling is weak, the aeroelastic characteristics of the blades can be determined from an isolated blade analysis.

Figures 6-1 and 6-2 show blade modal damping for the primary blade modes as function of forward speed at rotor speeds of 80%, 100%, and 110% N_R. Forward speed was accounted for by applying aerodynamic forces corresponding to the 90-degree azimuth position. A limiting condition of $\theta_{3/4} = 12^0$ and 3.5 g was used which is far higher than the GRMS capability. It can be seen that adequate stability margins are available.

Studies of this type, with the rotor in an axial flow mode of operation, will generally identify inherent design flaws that would lead to aeroelastic instabilities in forward flight in the pitch-lag, pitch-flap, and flap-lag categories. It is apparent that the model rotor is not susceptible to any of these which indicates a degree of aeroelastic similarity with the parent full scale AAH rotor which has been demonstrated to be free from instability.

The chordwise relationship among the elastic axis, center of pressure, and center of gravity for the model blades is similar to that of the full scale blades. The model blade torsional frequency is somewhat higher than full scale. These facts permit the conclusion that the model rotor will be free from advancing blade flutter and static torsional divergence for flight conditions representative of the full scale AAH main rotor.

7.0 LOADS -

It was shown in Section 5.0 that blade and rotor loads will not be significantly influenced by hub motions because of the weak dynamic coupling between the rotor and the GRMS. Therefore loads can be adequately defined using an isolated blade analysis. The DART analysis program used to compute the loads presented in this section is described in Reference 2. Aerodynamic interference effects between the rotor and GRMS were neglected.

Figures 7-1 through 7-3 show half peak-to-peak blade loads radial distribution for 1 g level flight. These figures compare AAH loads from flight test, Reference 6, with AAH analysis results, and results for the scaled model rotor. Note that model results are scaled up in order to be directly comparable with full scale results. Note that flapwise as well as chordwise bending moments are essentially the same for the full scale and the model rotor. The difference in the torsion loads, see Figure 7-3, can be attributed to the different control system stiffnesses.

Similar loads data to those described above are provided in Figures 7-4 through 7-5 for a 2.5 g maneuver. It is not anticipated that such a maneuver will be conducted in the wind tunnel; the data are provided only to give an indication of the upper limits of the capabilities of the rotor and to show comparison with flight test data.

8.0 AEROMECHANICAL STABILITY

Possibly the most fundamental instability associated with rotorcraft is that which has come to be known as "Ground Resonance". This description strictly is incorrect since the phenomenon is in fact, not a resonance but a true instability. A more appropriate name is "Mechanical Instability" which has seen more use in recent years. This is an appropriate description because the phenomenon can occur in a vacuum.

The classical works of Coleman and Feingold, Reference 7, and Deutsch, Reference 8, identified the rotorcraft parameters, and the relationships among those that are important to mechanical instability. Their works showed that the phenomenon is fundamentally simple but that the relationships required for stability among the parameters are very complex. They also showed that mechanical instability is possible only when the natural frequency of lagging (or inplane) motions of the rotor blades is less than the speed of rotation of the rotor.

In simple terms, mechanical instability can occur if:

- The lag frequency of the rotor blades is less than the rotor speed.

- The lag frequency minus the rotor speed (the regressive lag mode frequency) approaches, or coalesces with, the frequency of an airframe mode.

- There are certain relationships among:

  - Blade lag damping and airframe modal damping, and

  - Effective rotor mass and effective airframe modal masses.

For the scaled model AAH main rotor, the blade lag frequency is less than the rotor speed at 100% N_R. Therefore, to integrate the rotor with the GRMS,

mechanical stability must be considered. What follows describes the studies that were conducted to define and understand the stability characteristics.

Initial studies duplicated the model used in Reference 7. That is, the blades were assumed free to only lag, the hub was assumed free to only translate laterally (roll direction) and longitudinally (pitch direction), and air density was zero (vacuum). Blade lag damping was 9% critical at 100% N_R. The effective masses, frequencies, and dampings of the GRMS modes that were used were taken from the shake test data provided in Section 3.0. The modes that are important for mechanical stability are the gimbal pitch and motor roll modes because their frequencies and effective masses are within the ranges of concern. The vertical and lateral sting bending modes frequencies are sufficiently low, and the effective masses sufficiently high to reduce the rotor to GRMS coupling to insignificant levels.

Mechanical stability characteristics of this simplified system are shown in Figure 8-1. It can be seen that unstable coupling between the regressive lag mode and the GRMS motor roll mode is predicted to occur between 87% N_R and 104% N_R. It is also shown in this figure that the system can be stabilized by doubling the roll mode damping. Taken at face value, these results suggest that a further small increase in the roll mode damping would provide an adequate stability margin. It will be shown that this conclusion is erroneous and that more refined analysis is required to determine the stability characteristics of the coupled rotor/GRMS system.

The classical analysis of Coleman and Feingold, and that of the system described above, addressed the purely mechanical instability known as ground resonance with simplified models of the rotor and airframe (GRMS). Such simplified modeling has often proved to be adequate when applied to actual rotorcraft, but there are circumstances under which this approach is quite inadequate. The

model rotor/GRMS system is one such circumstance.

For a typical rotorcraft, the ratio of the effective rotor mass to that of the airframe roll mode (which is generally of most concern) is normally less than 0.1. For the model rotor/GRMS motor roll mode, this ratio is 0.3, whereas for the gimbal pitch mode, it is 0.07. Pitch or roll rotations of the hub that accompany hub translations in the important airframe modes of a typical rotorcraft are generally less than 0.02 radian/unit hub translation. For the GRMS, the roll and pitch rotations are respectively 0.063 and 0.074 radians/unit hub translation. A consequence of these rotations is that they cause blade flapping to participate much more in the model system than in the typical rotorcraft. The primary influence of thrust on an actual rotorcraft is to cause it to become partially, or wholly, airborne. Depending on the airframe modal properties, this can either degrade or improve stability. However, the effects are mainly due to changes in the dynamics of the airframe modes; thrust per se has only a minor influence. On the other hand, the model system cannot become airborne and thrust can have a significant influence on stability depending on the degree and phasing of flapping participation. Because of these considerations, it was decided that the analytical model of the rotor/GRMS system should include blade flapping as well as lagging, correct representation of the modal hub motions of the GRMS, rotor blade aerodynamic forces, and thrust effects. Rather than include all of these features simultaneously, a step-by-step approach was taken so that individual effects could be examined.

In the following discussions the baseline system will be that for which the data in Figure 8-1 were developed with 10.9% critical damping of the motor roll mode. The blade lag damping constant, not percent critical, is held constant with rotor speed.

The effects of adding aerodynamics (air density non-zero), and thrust to the baseline system are shown in Figure 8-2. It can be seen that simply adding aerodynamics, zero thrust has little influence while increasing thrust is stabilizing for this system. These results are not unexpected. Introducing aerodynamics alone essentially has only the effect of adding profile drag to the blades. This will be small compared to the blade damping from the lag dampers. Therefore, the in vacuo and in air characteristics should be similar. Increasing thrust adds induced drag which can be expected to augment lag damping and improve stability.

The influence of adding aerodynamics, thrust, and a flapping degree of freedom to the baseline system is shown in Figure 8-3. When compared to Figure 8-2, flapping is seen to have little influence on stability. In the absence of coning (zero thrust), the only forces that could cause the blades to flap result from blade angle of attack changes that are functions of the blade lag and hub inplane velocities. These velocities are small compared to those from rotor speed. Consequently, flapping will be small. Therefore, the addition of the flapping degree of freedom will have a negligible effect on stability. As the blades come under thrust, flapping caused by hub inplane accelerations will be induced by inertia forces on the coned blades. To illustrate the system behavior, the mode shape for the 1 g thrust configuration at the point of minimum stability is shown in Figure 8-4. This shows that the pattern of the blade lag motions is that classically associated with ground resonance. That is, the center of gravity of the rotor when viewed from above is moving in a retrograde sense in rotating axes -- opposite to the direction of rotor rotation. The instant in time shown is when the lateral (roll) flapping is maximum. Maximum lateral flapping occurs at this instant which causes the thrust vector to tilt through an angle equal to the flapping angle, thereby

introducing a component acting in the plane of the hub. This component of thrust acts against the hub velocity, and provides a measure of positive damping, but this is somewhat washed out by the Coriolis forces from blade flapping which provide negative damping. For the mode under consideration, all of these effects are relatively small because the flapping participation is small (flapping is only about one-tenth of the lag amplitude), therefore the stability characteristics are similar to those for the system with no flapping degree of freedom, Figure 8-2. The mode shape does, however, illustrate how factors other than those classically considered can enter into the picture.

The influence of adding a flapping degree of freedom and allowing the hub to pitch and roll while translating longitudinally and laterally, respectively, is shown in Figure 8-5 for a vacuum environment. Two effects are seen. First, the roll frequency increases with increasing rotor speed which causes coalescence with the regressive lag mode to occur at a higher rotor speed. Second, the system is destabilized. Part of the destabilizing influence can be traced to the fact that the blade lag damping constant is held constant with rotor speed. This means that the percent critical lag damping decreases with increased rotor speed. Also damping required for stability increases as the rotor speed at coalescence increases largely due to the increased rotor energy available.

The mode shape for this configuration at the point of minimum stability when the lateral (roll) flapping is maximum is shown in Figure 8-6. Not surprisingly, it is apparent that hub rotations cause the blades to flap (rotate) about their centers of percussion. The resulting inertia forces at the blade flapping hinge offset cause a moment that acts against the hub rotation, and therefore hub displacement, to effectively increase the roll stiffness. This stiffening effect increases with increasing rotor speed which explains the frequency trend seen in Figure 8-5. It should be pointed out that the effect

observed here is significant only because the GRMS has an unusually high rotor to roll mode effective mass ratio and unusually large hub rotations that accompany lateral motions of the hub in the roll mode. Although the flapping hinge offset is low, these features of the model system make it more sensitive to the hub moments caused by blade flapping than would be the case for a typical rotorcraft with a similar low hinge offset.

The combined influence of aerodynamics, thrust, flapping degree of freedom, and hub pitch and roll is shown in Figure 8-7. Two effects are seen. First, increasing thrust increases the frequency separation between the roll and regressing lag mode at coalescence. This indicates a stronger coupling between these modes and, typically, a lesser degree of stability. Second, the system is destabilized in proportion to the amount of thrust developed by the rotor.

The mode shape for this configuration at the point of minimum stability is shown in Figure 8-8. From this it is seen that the source of negative damping comes directly from thrust. Examining the phasing between flapping and rolling proves this point. The instant in time shown is when the lateral (roll) flapping is maximum. The thrust vector, being perpendicular to the tip path plane, thus tilts through an angle equal to and in phase with the flapping angle. The resulting thrust component in the plane of the hub acts in phase with the hub inplane velocity and thus provides a destabilizing force. The measure of negative damping is directly proportional to the flapping amplitude and the amount of thrust. Comparing Figure 8-8 with 8-4 shows that the phasing between flapping and hub lateral motion is changed unfavorably when the hub rotational degrees of freedom are included. These studies are evidence that a simplified model does provide erroneous results in the situation at hand.

From Figure 8-7 it is evident that the 0.27 scale AAH rotor/GRMS system

will be unstable at operating RPM. A series of investigations was performed to identify possible changes of the system parameters that would eliminate this instability. Since it is desirable to maintain the model rotor properties as close as possible to those of the full scale rotor only GRMS changes were considered. By design, the GRMS roll and pitch springs and dampers can be varied. Consequently, the effect of these parameters was studied. The results can be summarized as follows. Changes to the GRMS pitch frequency and damping have little effect. This is not surprising, since it is the roll mode that couples with the regressing lag mode. Any increase in GRMS roll mode damping will be helpful, see Figure 8-9. A considerable increase in roll frequency (above 1.5 * nominal) would be required to provide sufficient stability margins, see Figure 8-10. A decrease in roll frequency seems to be more effective. Figure 8-11 shows that lowering the roll frequency to 0.75 * nominal adds considerable damping to the system. A possible solution to the ground resonance instability would therefore be to reduce the roll frequency and increase the roll damping of the GRMS.
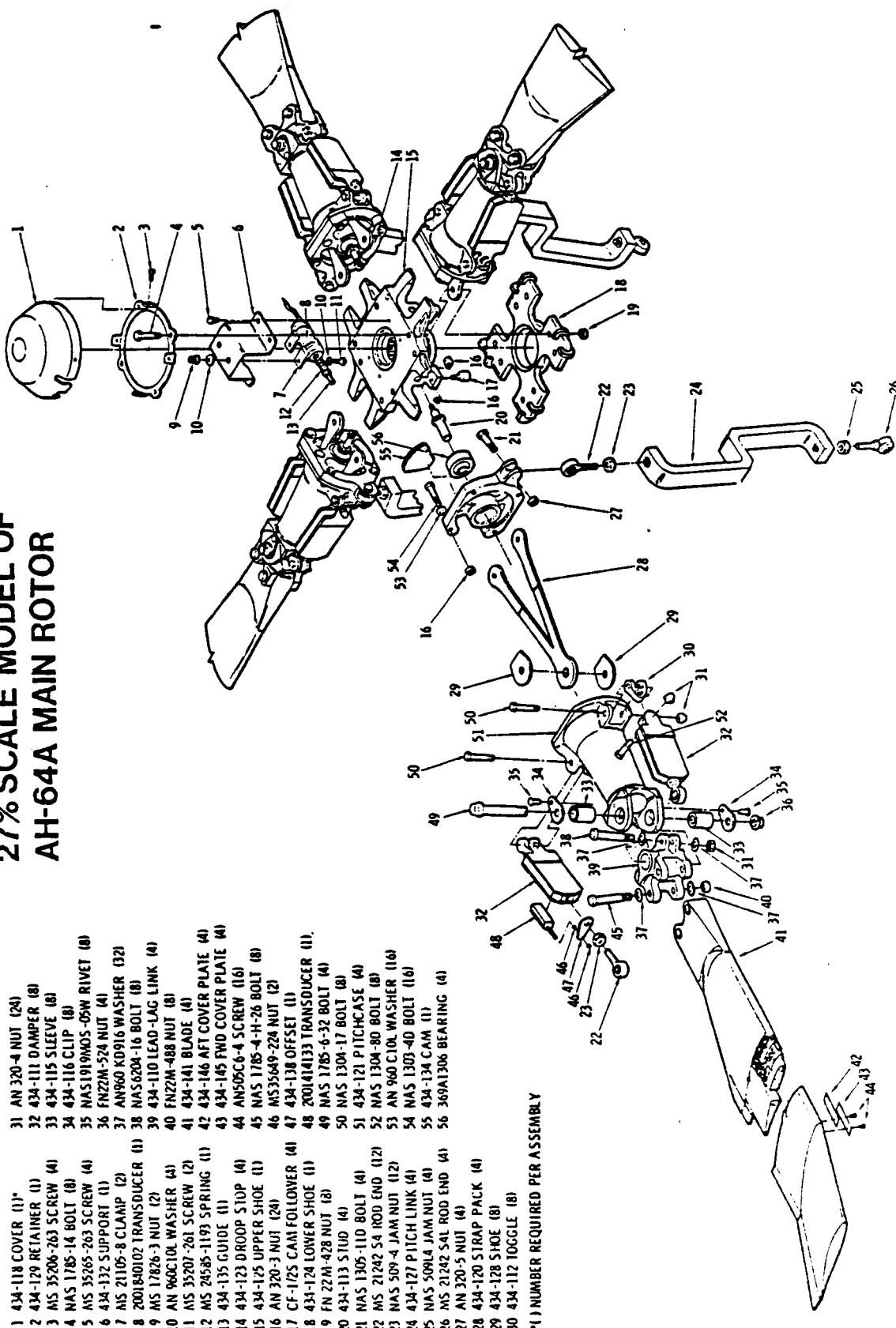
All ground resonance results shown here were computed using the E-927 computer analysis. An independent study, using the DART analysis, confirmed that the combined effects of flapping, thrust, and hub rotations destabilize the system. The results obtained with DART were very similar to those from E-927, but generally more conservative (due to the isotropic hub support model).

REFERENCES

1. Murrill, R. J. "Operation and Maintenance Manual for the General Rotor Model System," NASA CR-145230, May 1977.

2. MacNeal-Schwendler Corp., "Theoretical Basis for SADSAM Computer Program," MSR-11, 1973.

3. Johnston, R. A. and Cassarino, S. J., "Aeroelastic Rotor Stability Analysis," USAAMRDL-TR-75-40, January 1976.

4. Straub, F. K., "NASA Langley Research Center General Rotor Model System Shake Test Report," Hughes Helicopters Report No. 150-V-1002, November 1981.

5. Oliva, T. J., "Test Report for the Control System Proof Load and Operation Demonstration, YAH-64 Advanced Attack Helicopter," Hughes helicopters Report No. 77-BT-5201-2, March 1979.

6. Harris, W. D., "Basic Loads Report for the YAH-64 Advanced Attack Helicopter, Volume II, Rotor, Controls, and Drive System Loads," Hughes Helicopters Report No. 77-S-8000-2, April 1981.

7. Coleman, R. P., "Theory of Self-Excited Mechanical Oscillations of Hinged Rotor Blades," NACA ARR No. 36, July 29, 1943. (Subsequently reissued under authorship of R. P. Coleman and A. M. Feingold as NACA TR 1351, 1958.

8. Deutsch, M. L., "Ground Vibrations of Helicopters," Journal of the Aeronautical Sciences, May 1946.

9. Ormiston, R. A., "Aeromechanical Stability of Soft Inplane Hingeless Rotor Helicopters," Paper No. 25, Third European Rotorcraft and Powered Lift Aircraft Forum, Aix-En-Provence, France, 1977.

27% SCALE MODEL OF AH-64A MAIN ROTOR

1	434-118 COVER (1)*	31 AN 320-4 NUT (24)
2	434-129 RETAINER (1)	32 434-111 DAMPER (8)
3	MS 35206-263 SCREW (4)	33 434-115 SLEEVE (8)
4	NAS 1785-14 BOLT (8)	34 434-116 CLIP (8)
5	MS 35265-263 SCREW (4)	35 NAS1919MOS-05W RIVET (8)
6	434-132 SUPPORT (1)	36 FN22M-524 NUT (4)
7	MS 21105-8 CLAMP (2)	37 AN960 KD916 WASHER (32)
8	200184D102 TRANSDUCER (1)	38 NAS6204-16 BOLT (8)
9	MS 17826-3 NUT (2)	39 434-110 LEAD-LAG LINK (4)
10	AN 960C10L WASHER (3)	40 FN22M-488 NUT (8)
11	MS 35207-261 SCREW (2)	41 434-141 BLADE (4)
12	MS 24565-1193 SPRING (1)	42 434-146 AFT COVER PLATE (4)
13	434-135 GUIDE (1)	43 434-145 FWD COVER PLATE (4)
14	434-123 DROOP STOP (4)	44 AN505C6-4 SCREW (16)
15	434-125 UPPER SHOE (1)	45 NAS 1785-4-H-26 BOLT (8)
16	AN 320-3 NUT (24)	46 MS35649-224 NUT (2)
17	CF-1/25 CAM FOLLOWER (4)	47 434-138 OFFSET (1)
18	431-124 LOWER SHOE (1)	48 200141133 TRANSDUCER (1)
19	FN 22M-428 NUT (8)	49 NAS 1785-6-32 BOLT (4)
20	434-113 STUD (4)	50 NAS 1304-17 BOLT (8)
21	NAS 1305-11D BOLT (4)	51 434-121 PITCHCASE (4)
22	MS 21242 S4 ROD END (12)	52 NAS 1304-80 BOLT (8)
23	NAS 509-4 JAM NUT (12)	53 AN 960 C10L WASHER (16)
24	434-127 PITCH LINK (4)	54 NAS 1303-40 BOLT (16)
25	NAS S09L4 JAM NUT (4)	55 434-134 CAM (1)
26	MS 21242 S4L ROD END (4)	56 369A1306 BEARING (4)
27	AN 320-5 NUT (4)	
28	434-120 STRAP PACK (4)	
29	434-128 SHOE (8)	
30	434-112 TOGGLE (8)	

*( ) NUMBER REQUIRED PER ASSEMBLY

FIGURE I-1: EXPLODED VIEW OF THE MODEL ROTOR
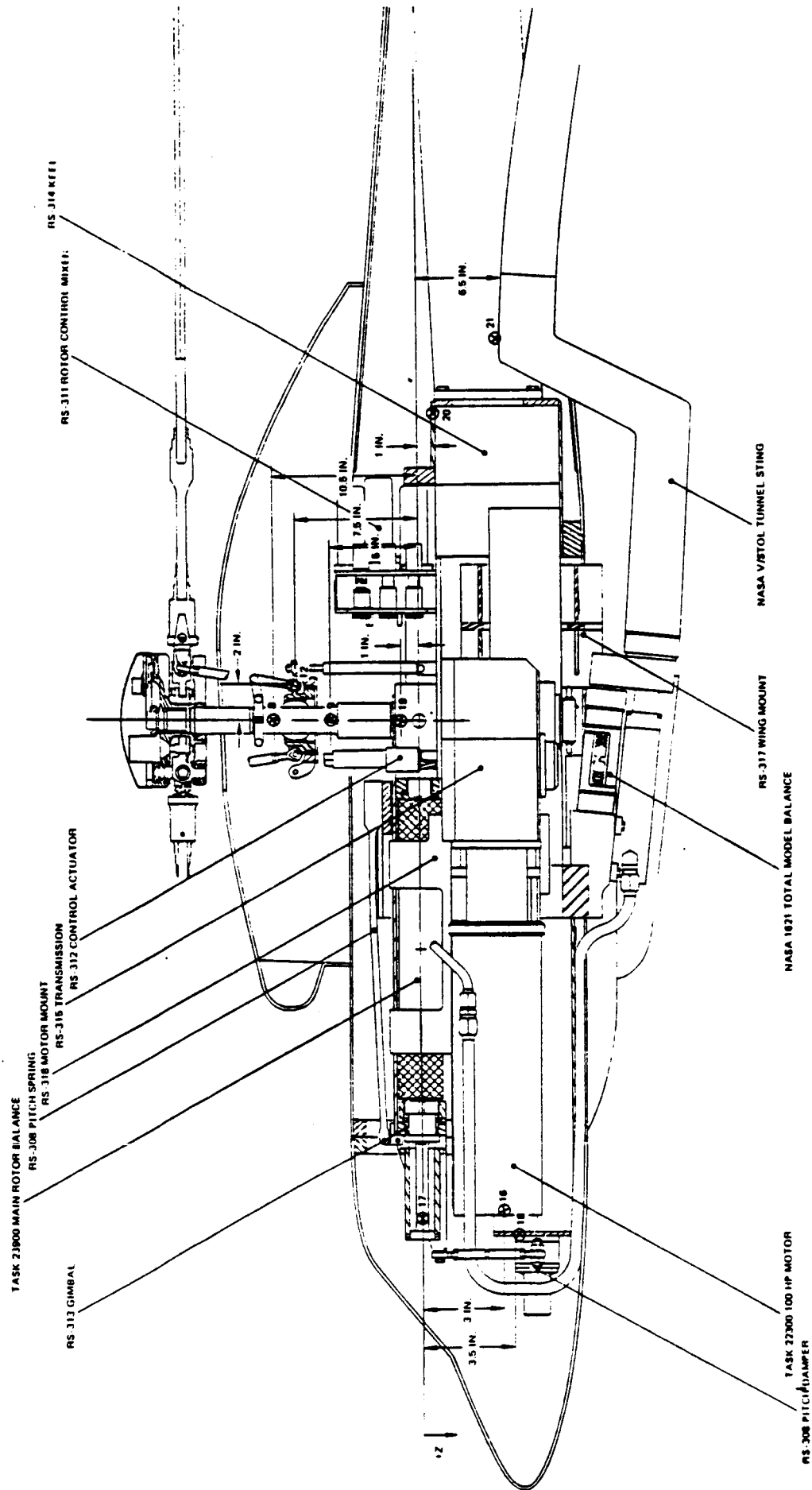
FIGURE I-2: GENERAL ROTOR MODEL SYSTEM (GRMS)
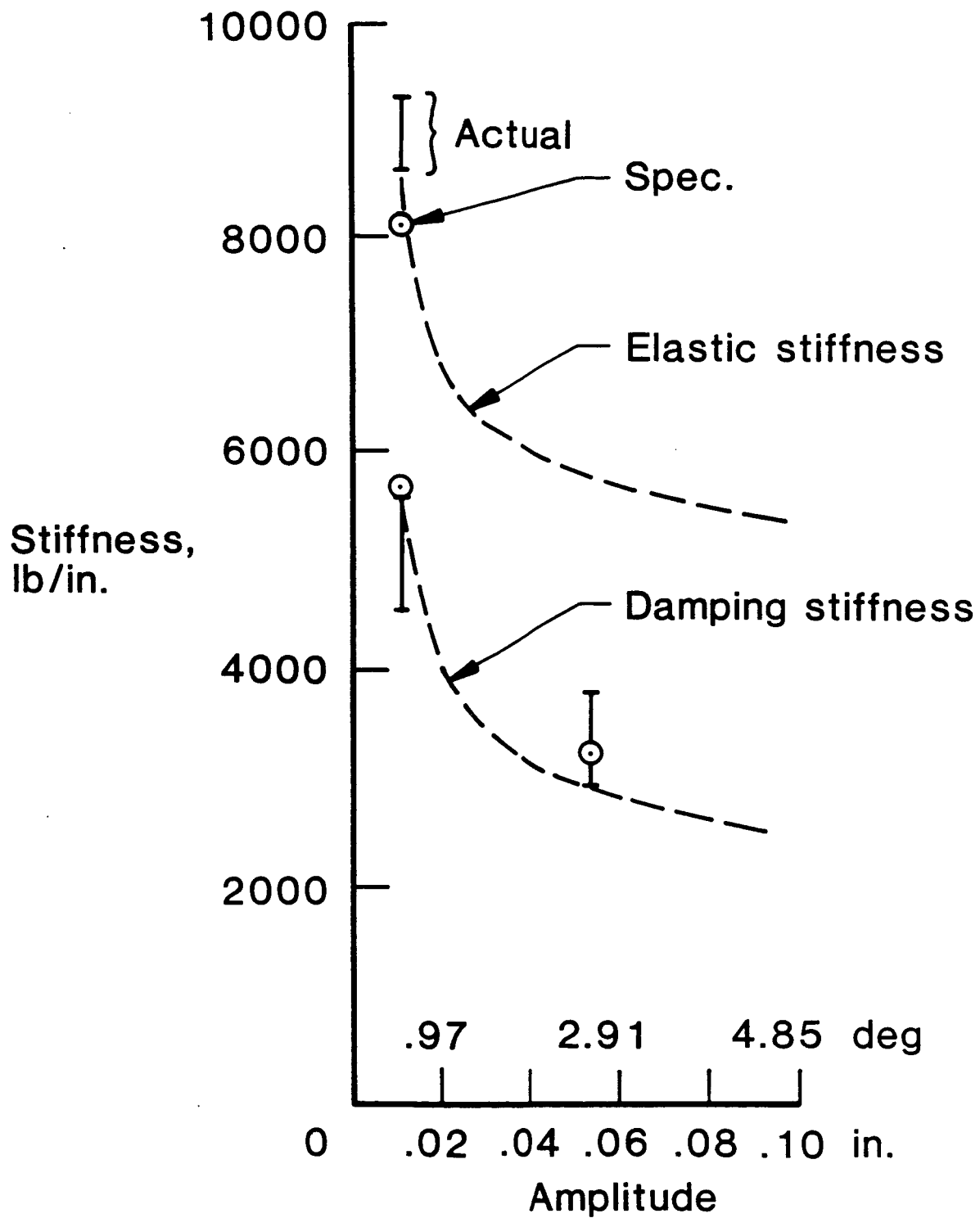
FIGURE 2-1: EFFECT OF AMPLITUDE ON LAG DAMPER 0.27 SCALE ROTOR
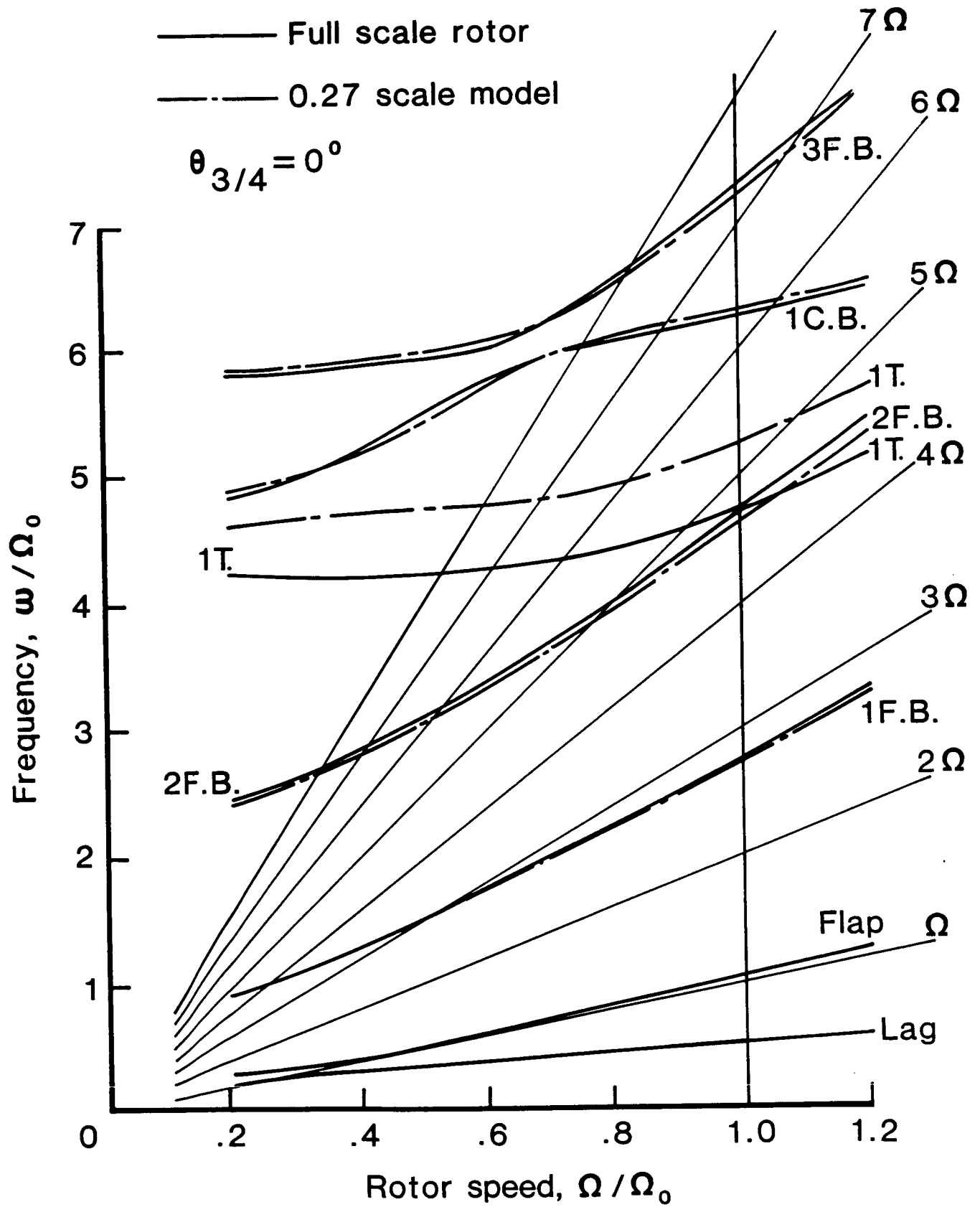
FIGURE 4-1: ISOLATED BLADE FREQUENCIES
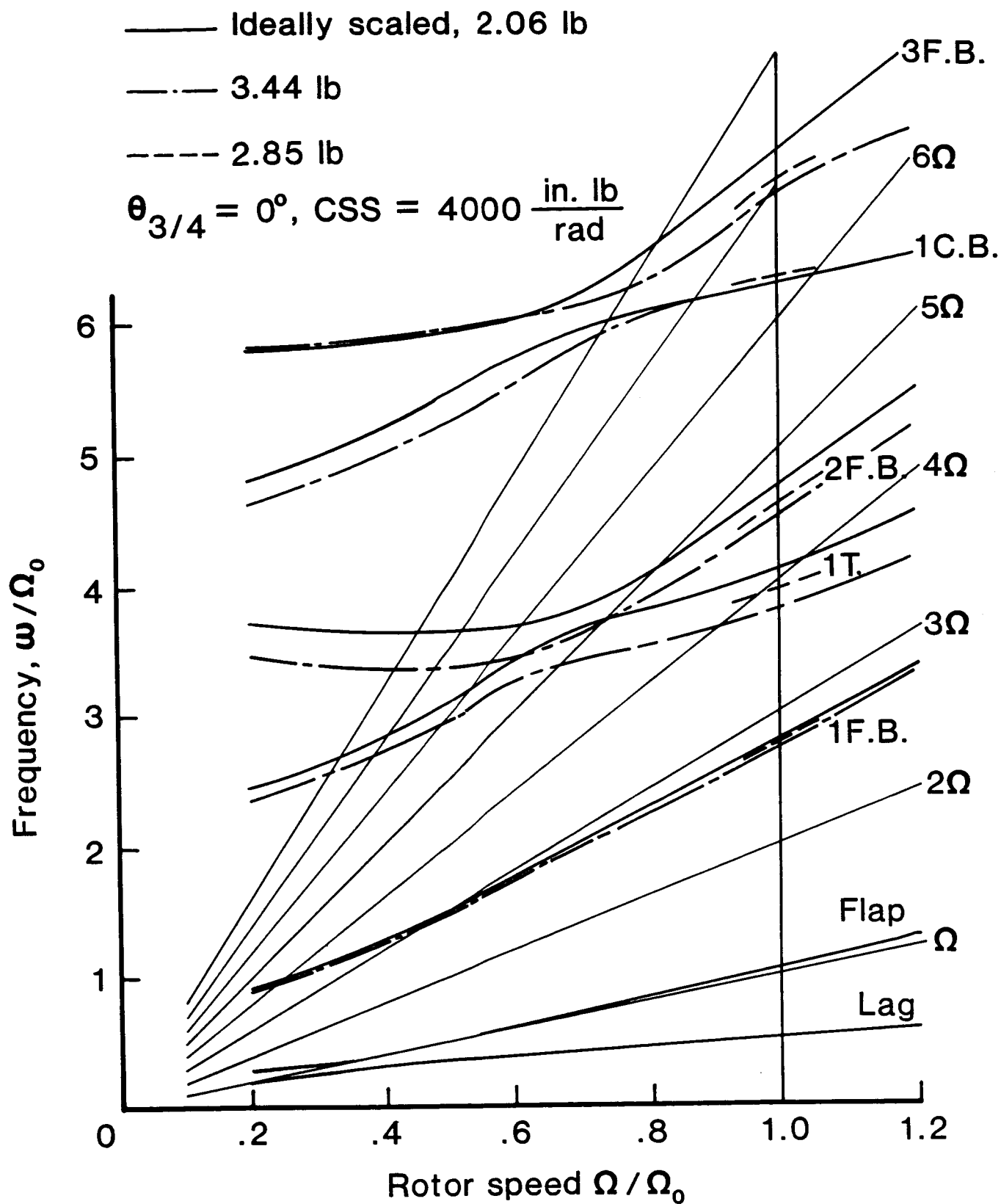
FIGURE 4-2: EFFECT OF FLAPPING HARDWARE WEIGHT ON ISOLATED BLADE FREQUENCIES
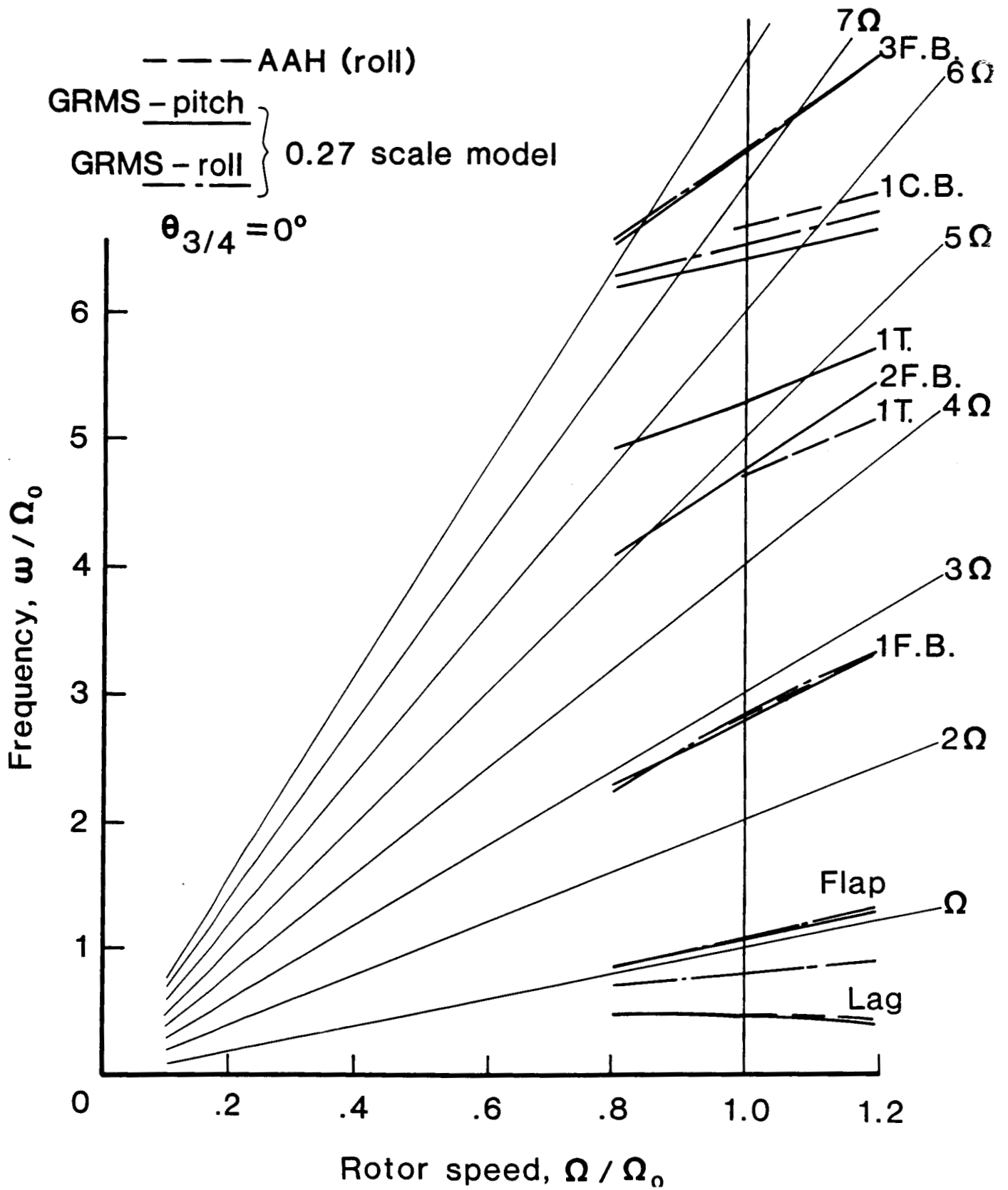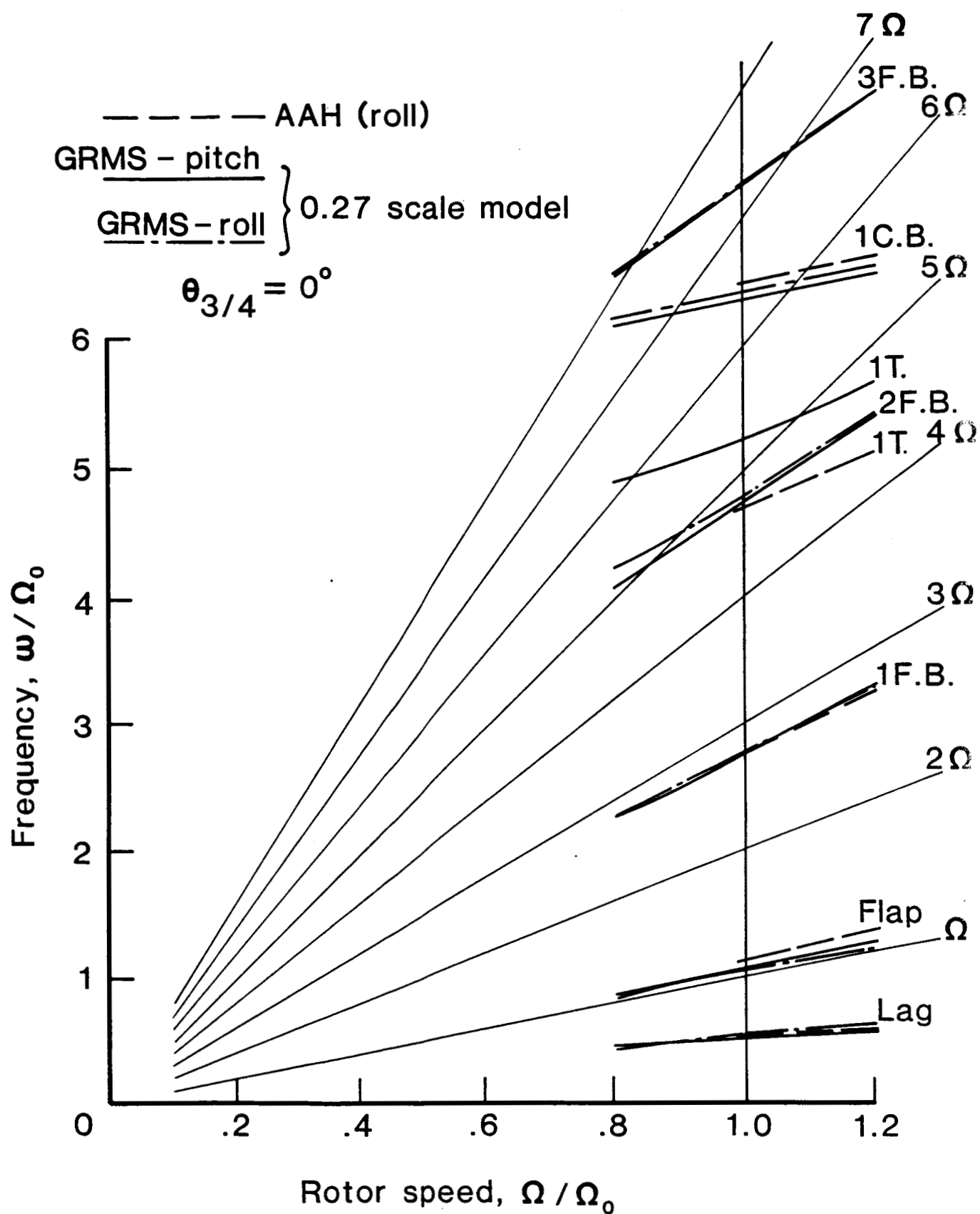
FIGURE 5-1: COUPLED ROTOR/GRMS ADVANCING CYCLIC MODES
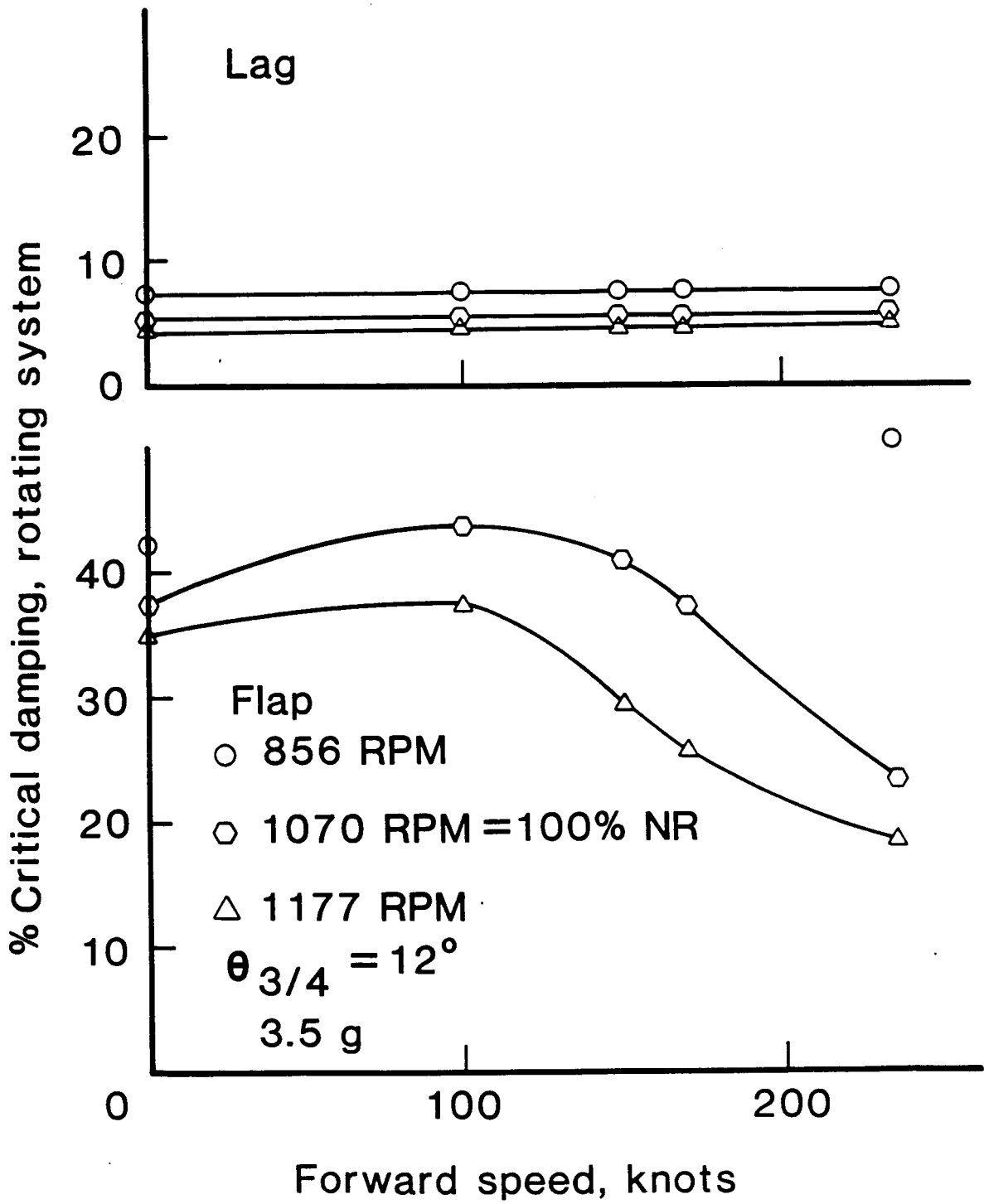
FIGURE 5-2: COUPLED ROTOR/GRMS REGRESSING CYCLIC MODES

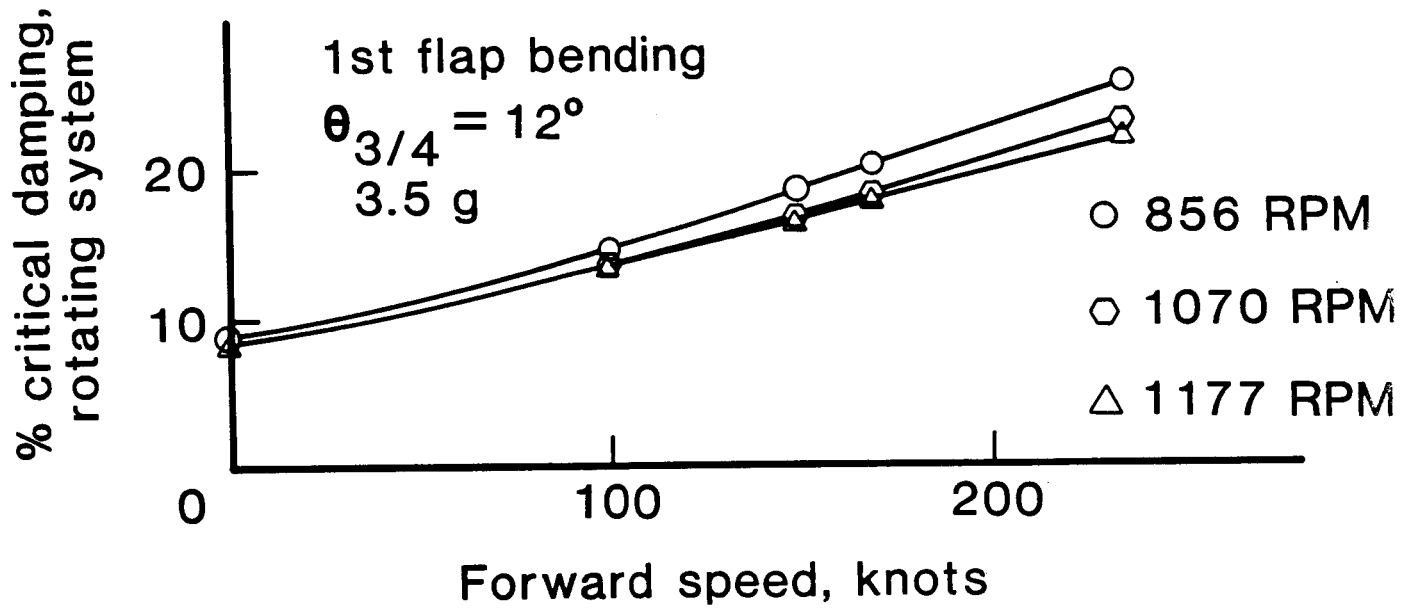FIGURE 6-1: .27 SCALE ROTOR BLADE DAMPING VS. FORWARD SPEED, ISOLATED BLADE
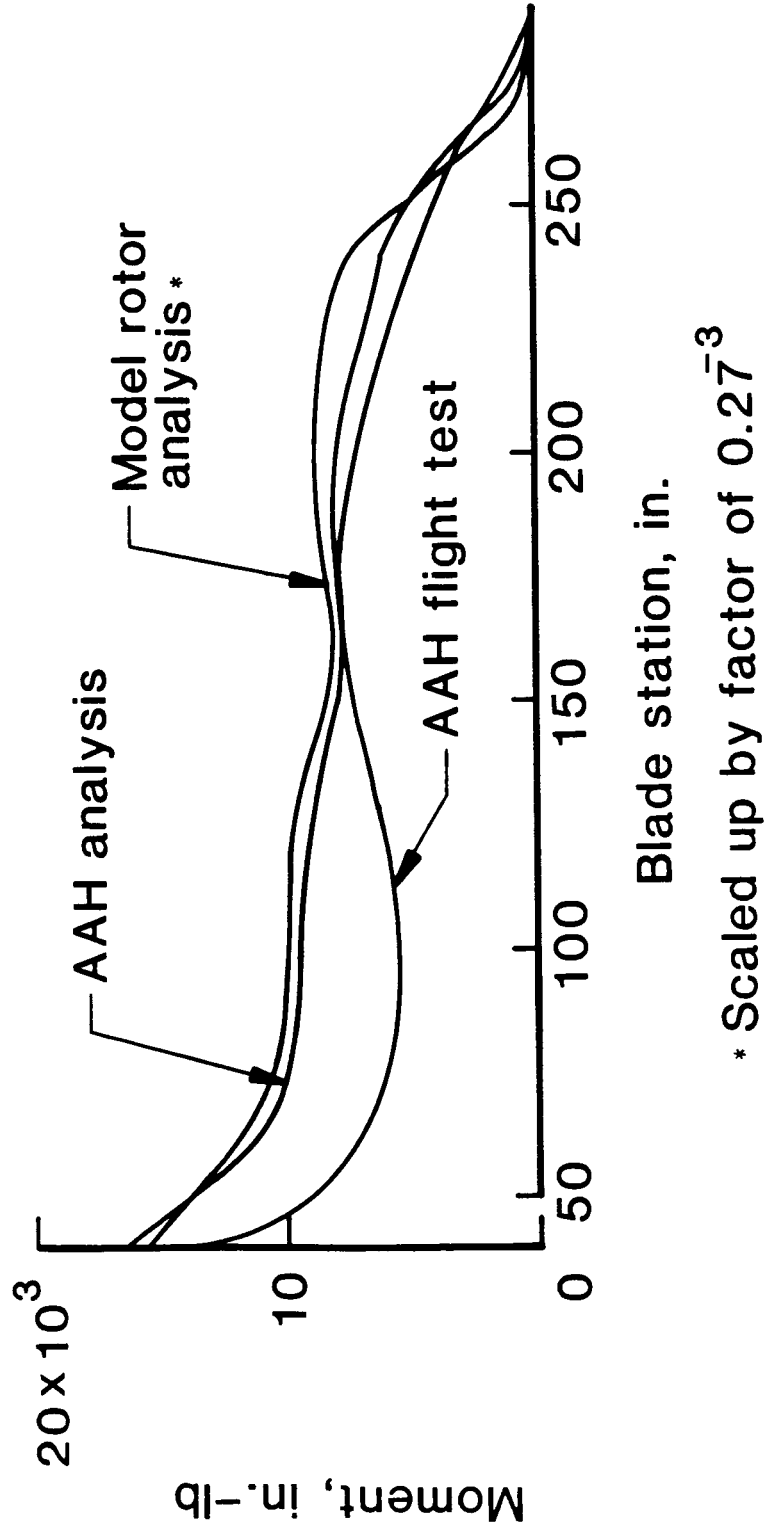
FIGURE 6-2: .27 SCALE ROTOR BLADE DAMPING VS. FORWARD SPEED ISOLATED BLADE

FIGURE 7-1: M/R BLADE BEDING MOMENT, 1/2 PP FLAPWISE BENDING ~ 1.0 G (164 KNOTS)
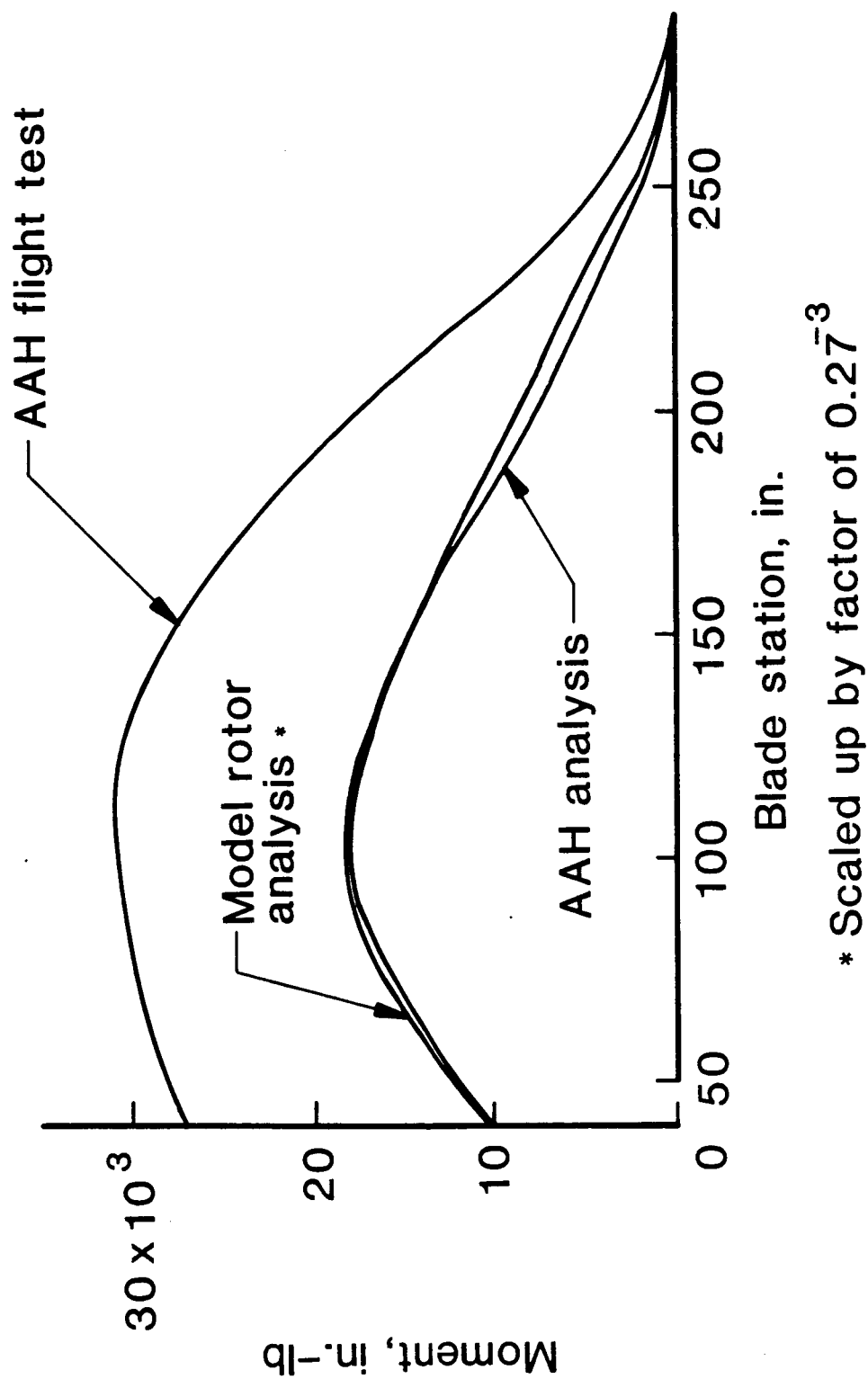
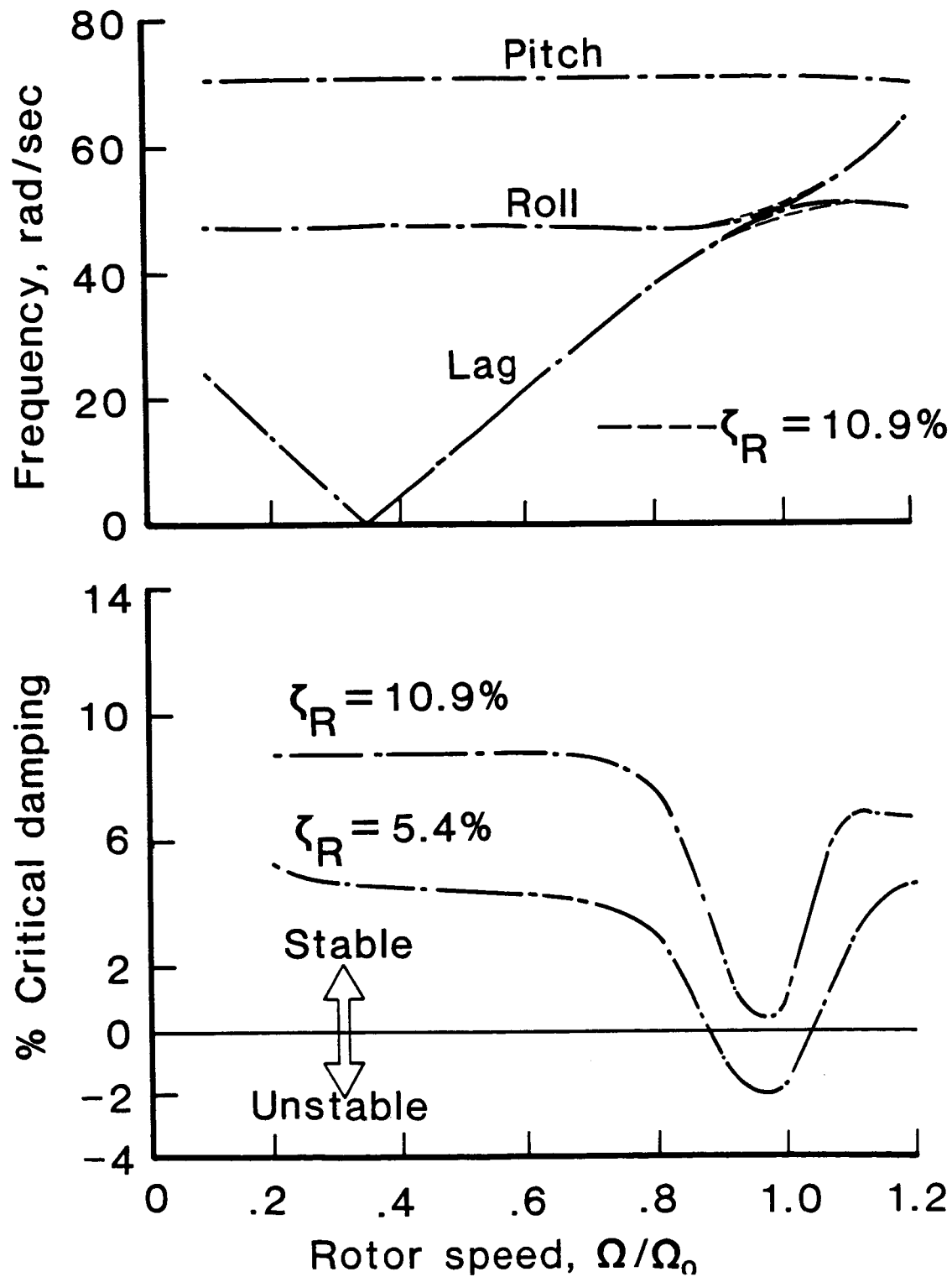FIGURE 7-2: M/R BLADE BENDING MOMENT, 1/2 PP CHORDWISE BENDING ~ 1.0 G (164 KNOTS)
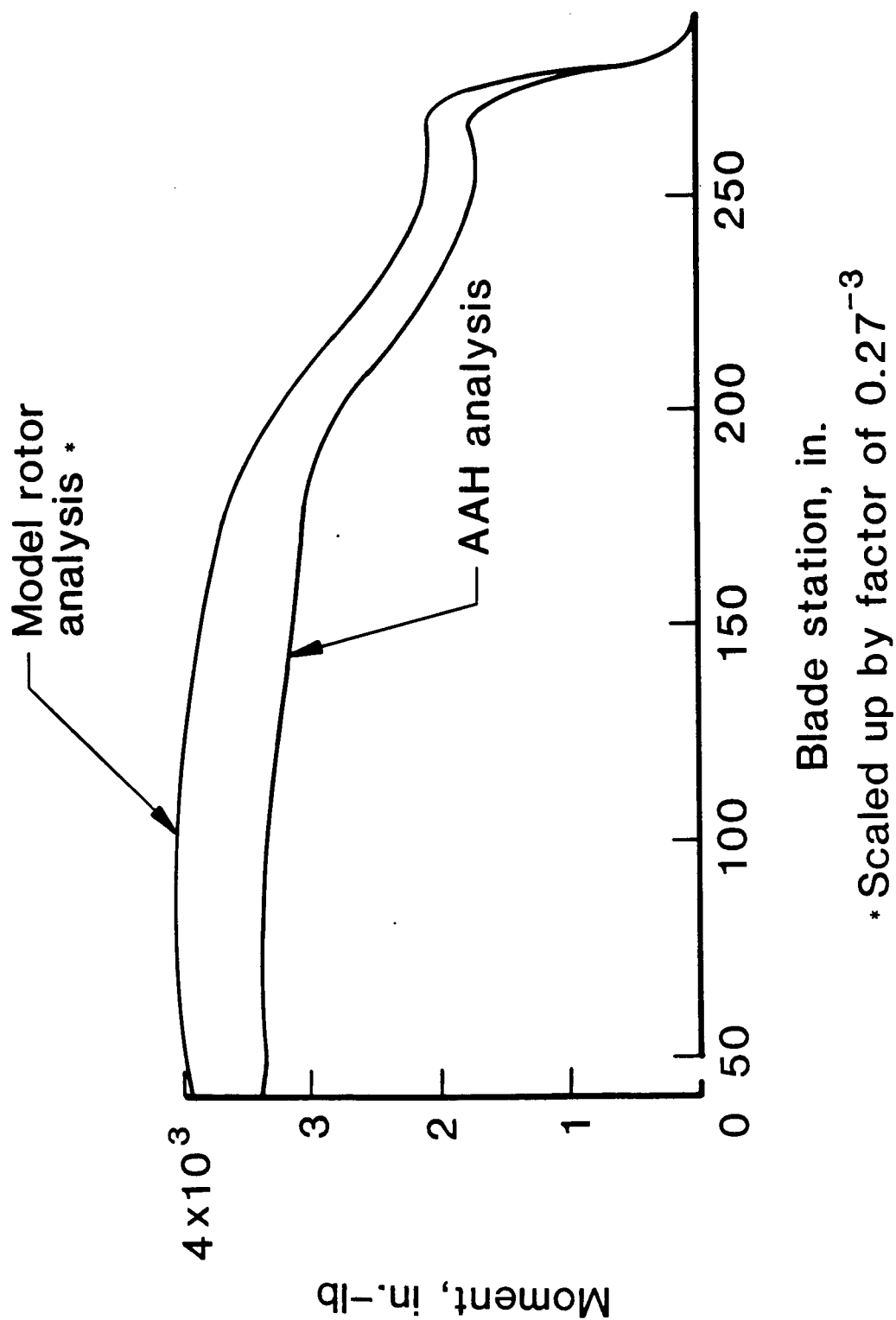
FIGURE 7-3: M/R BLADE MOMENT, 1/2 PP TORSION -1.0 G (164 KNOTS)
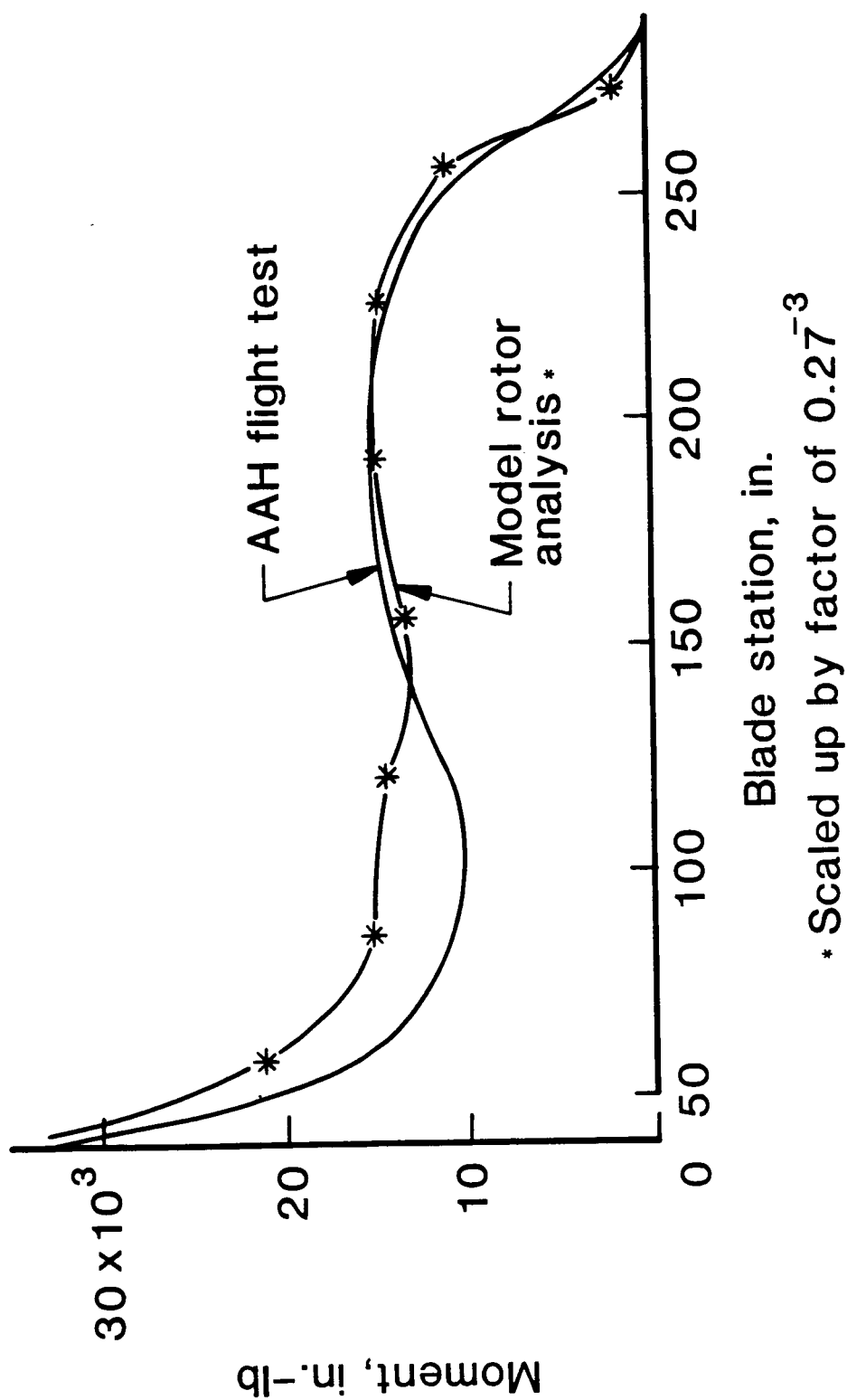
FIGURE 7-4: M/R BLADE BENDING MOMENT, 1/2 PP FLAPWISE BENDING - MANEUVERS 2.5
G (164 KNOTS)
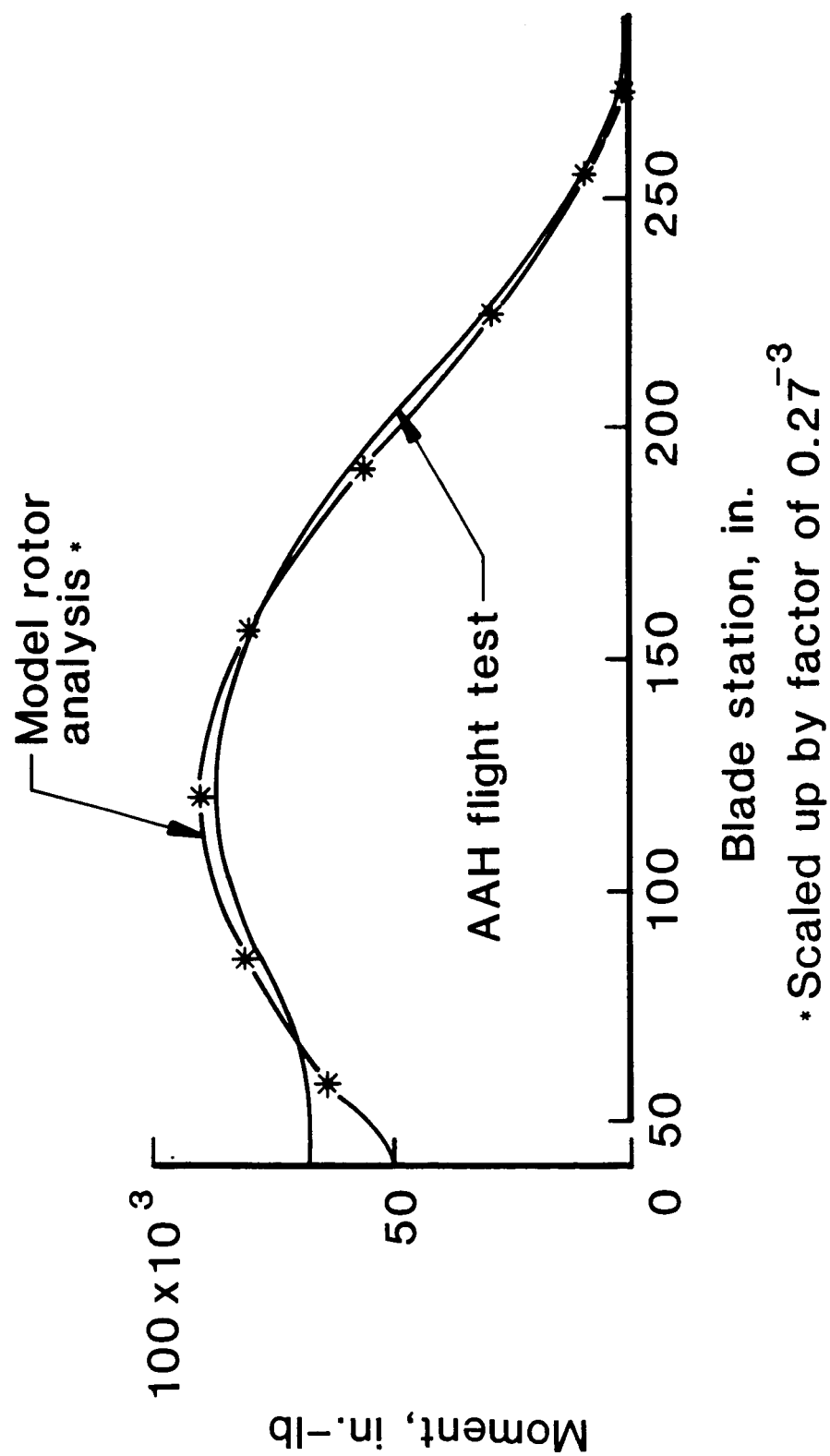
FIGURE 7-5: M/R BLADE BENDING MOMENT, 1/2 PP CHORDWISE BENDING – MANEUVERS
2.5 G (164 KNOTS)

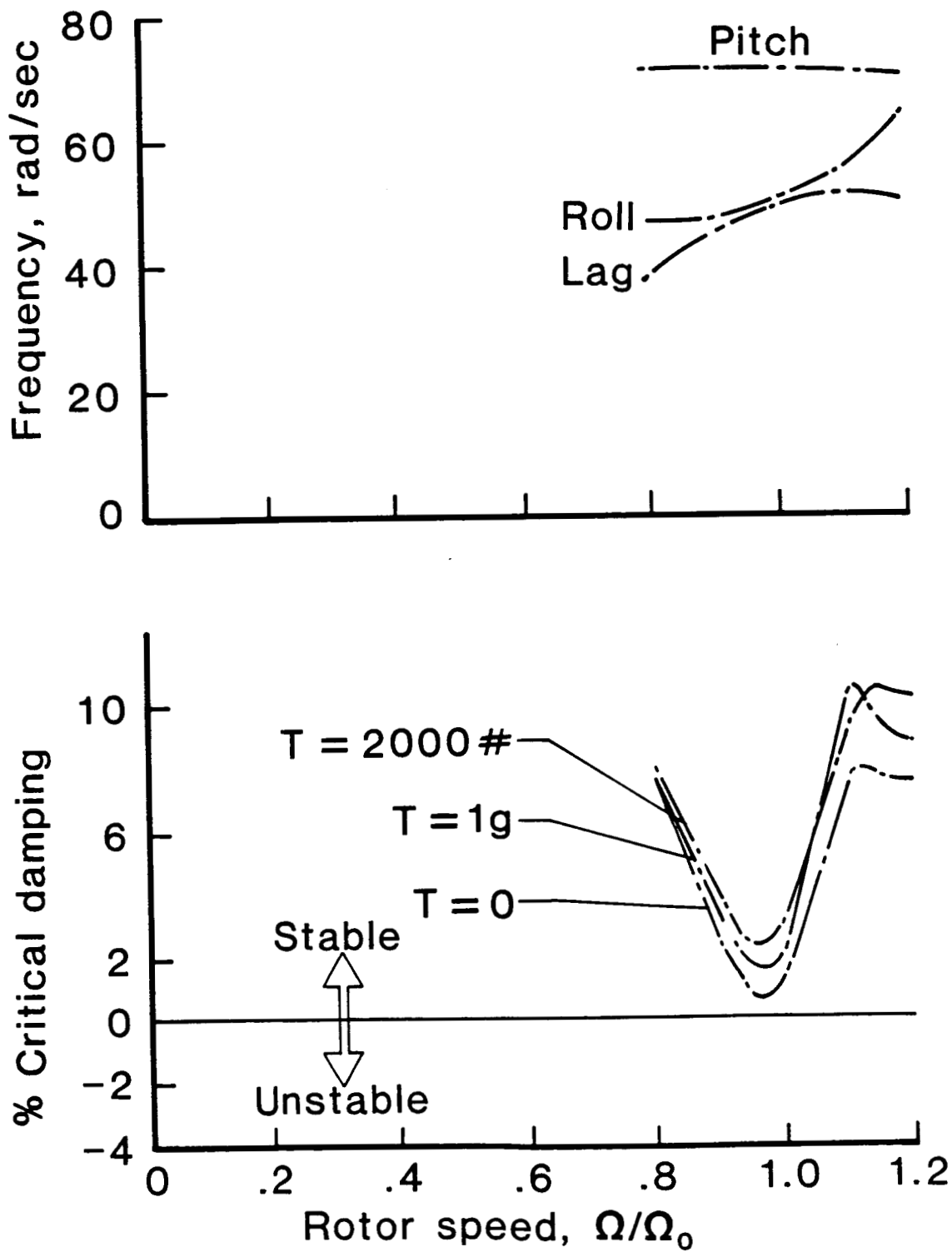FIGURE 8-1: 0.27 SCALE ROTOR/GRMS GROUND RESONANCE CLASSICAL ANALYSIS
(δ = 0, LAG)

FIGURE 8-2: GROUND RESONANCE, EFFECTS OF THRUST (δ = AIR, ζ_R = 10.9%, LAG)

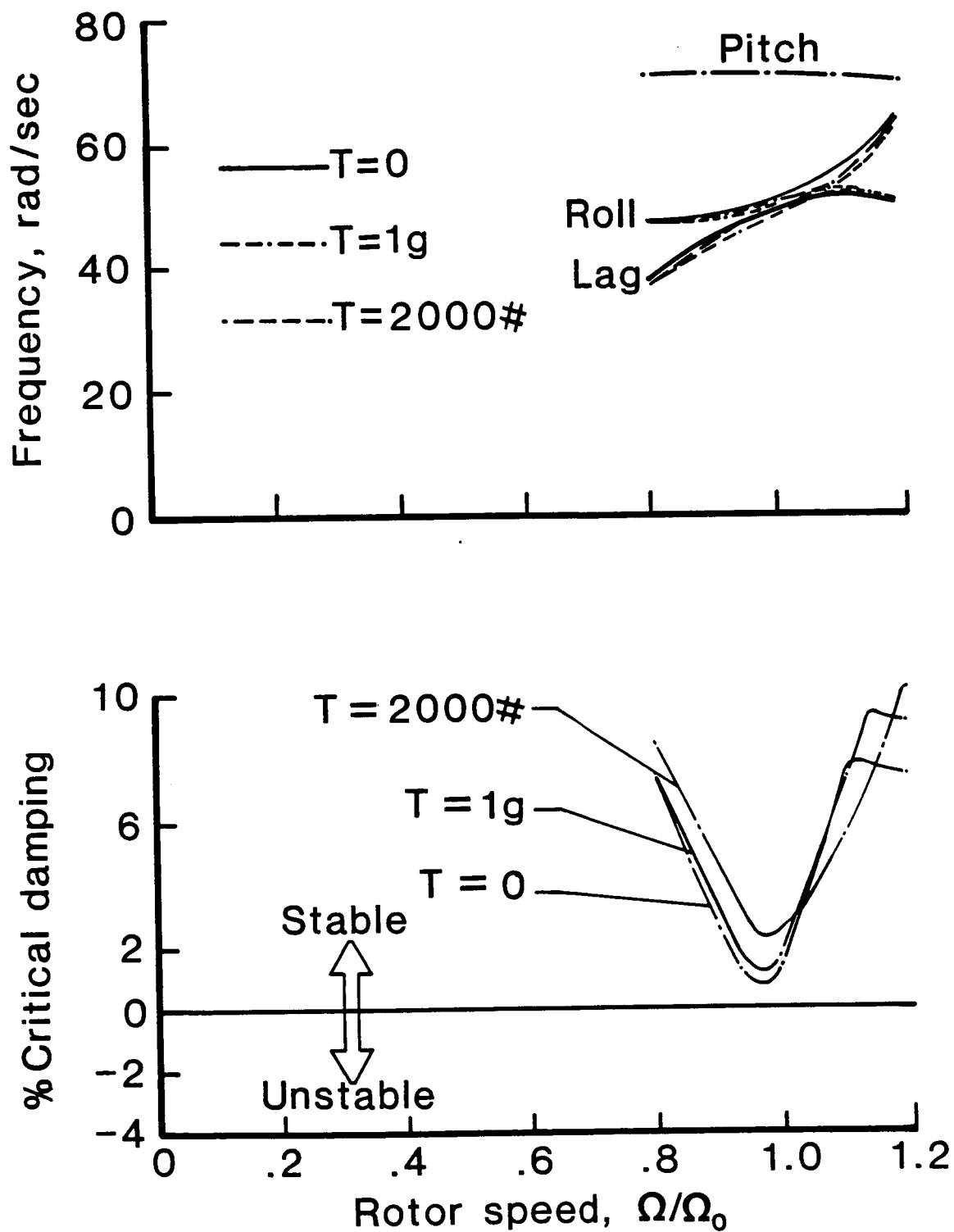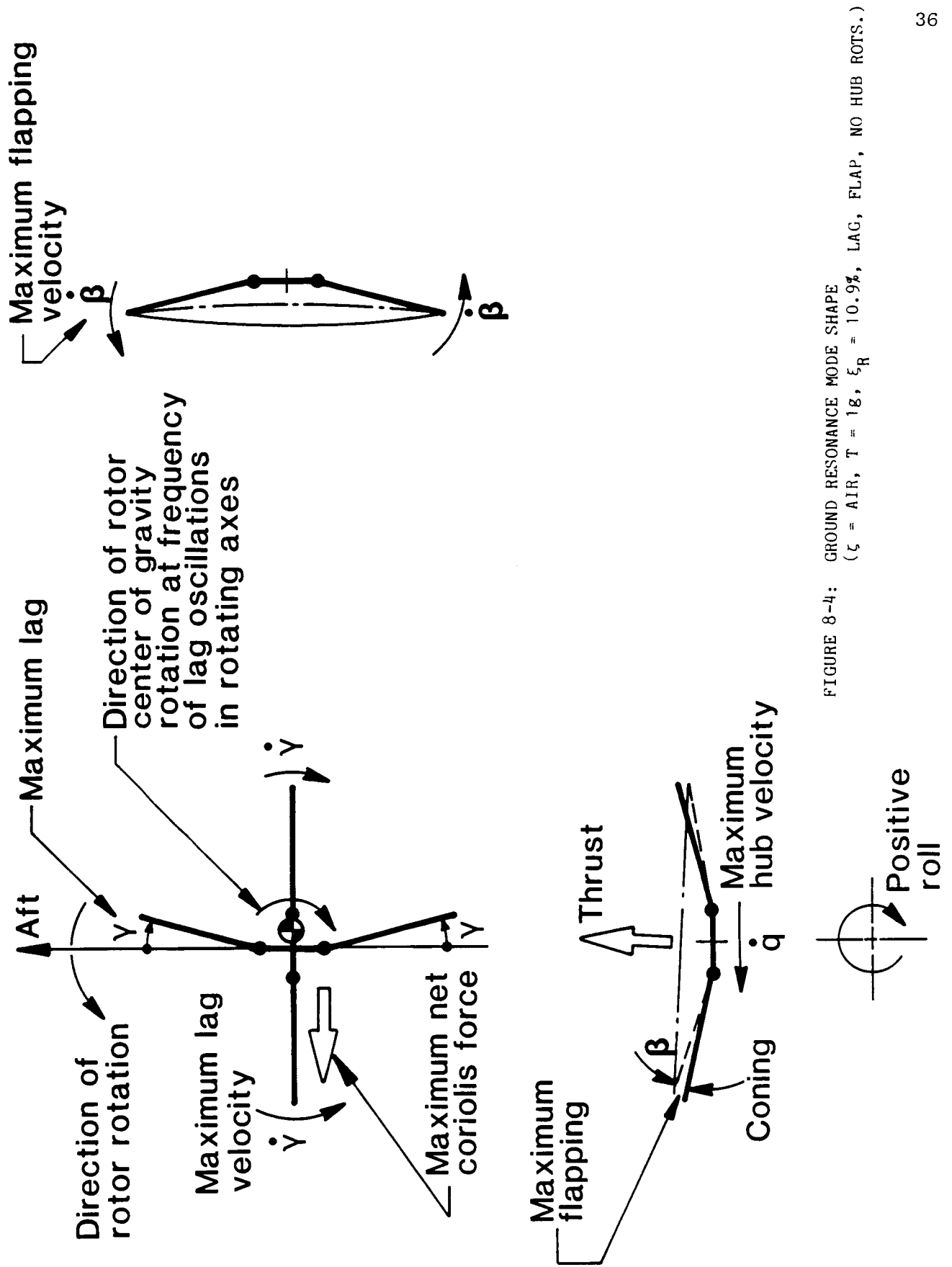FIGURE 8-3:   GROUND RESONANCE WITH FLAPPING (ζ = AIR, ξ_R = 10.9%, LAG, FLAP)

FIGURE 8-4: GROUND RESONANCE MODE SHAPE
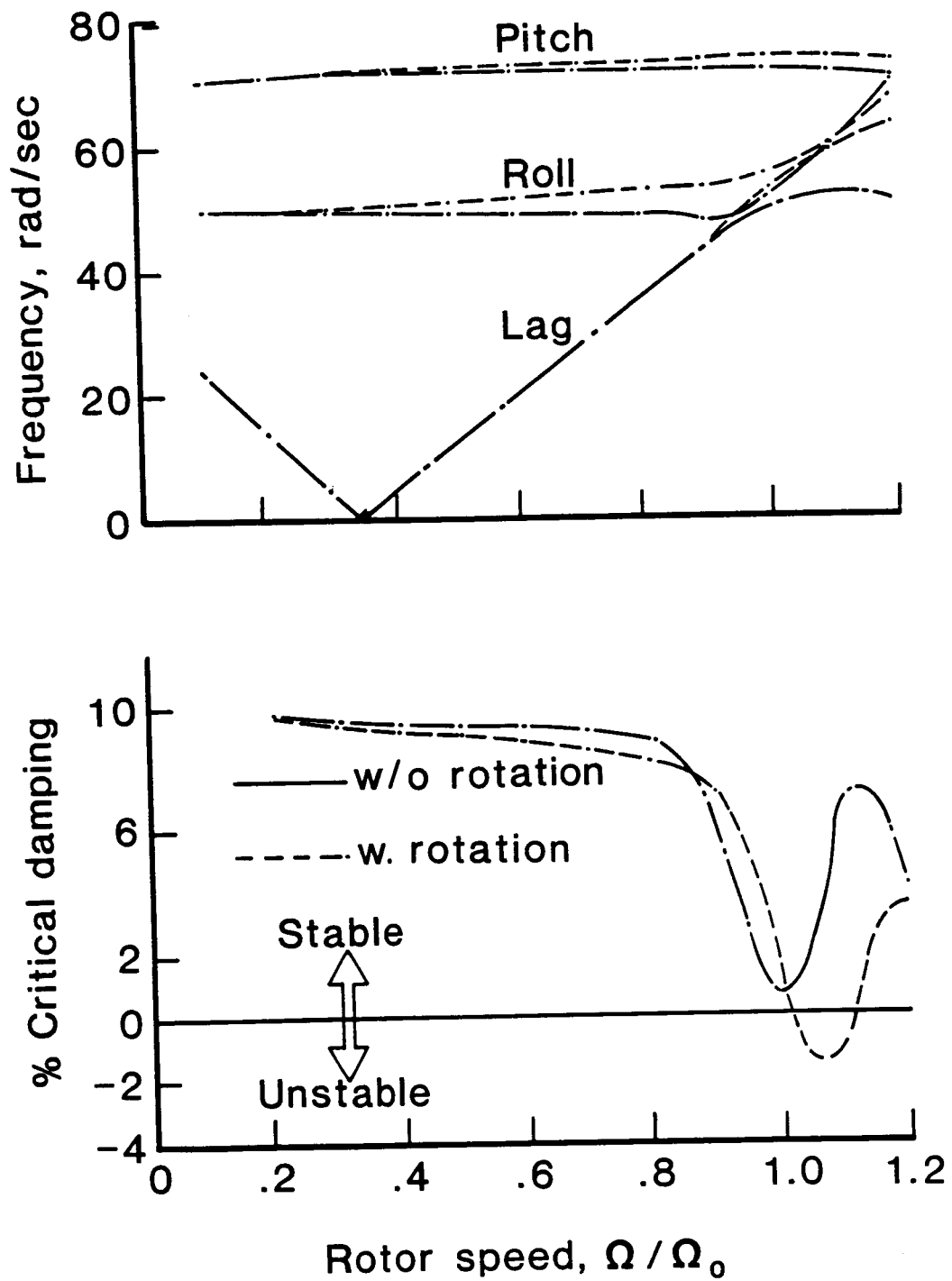(ζ = AIR, T = 1g, ξ_R = 10.9%, LAG, FLAP, NO HUB ROTS.)

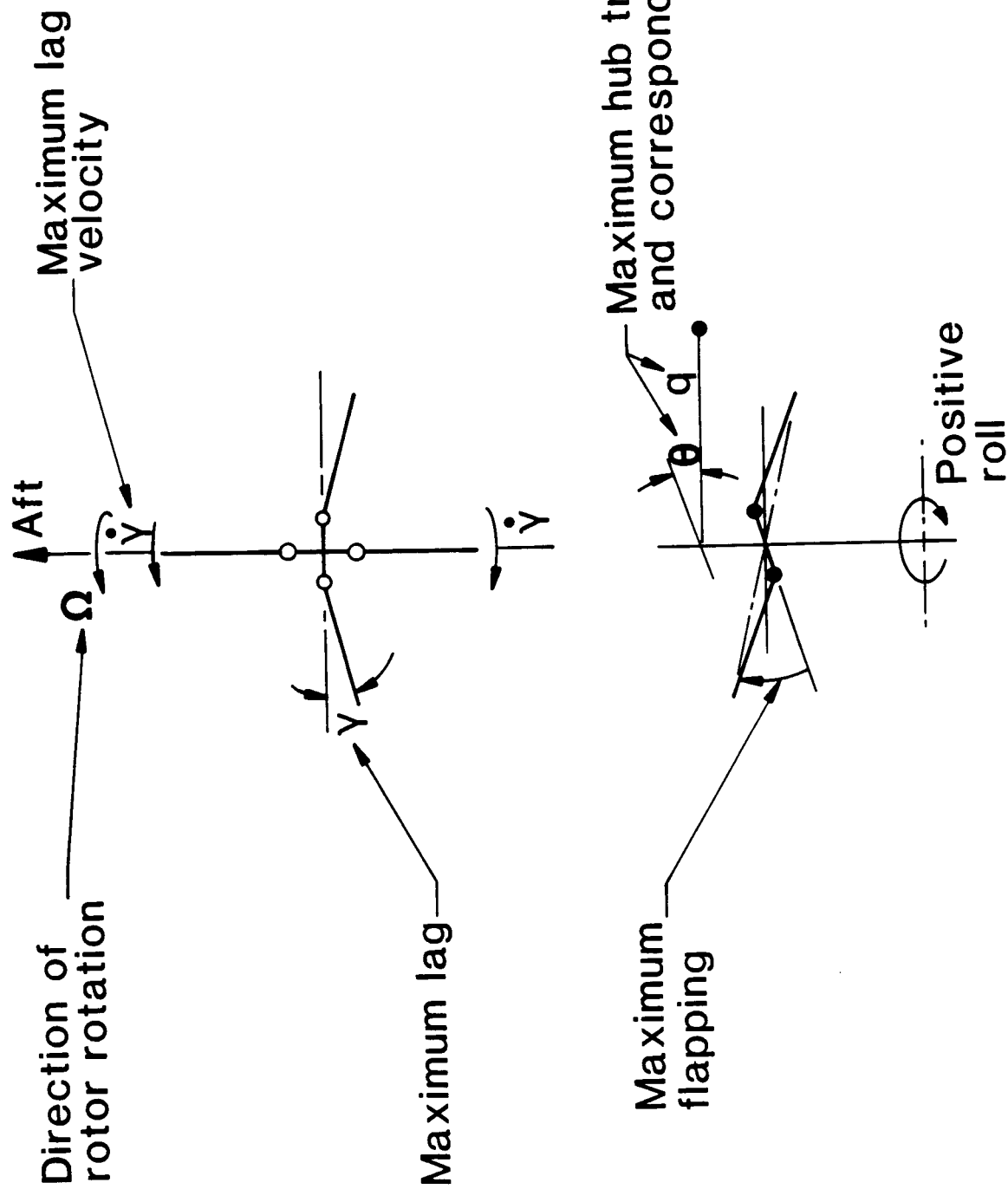FIGURE 8-5: GROUND RESONANCE EFFECTS OF HUB ROTATIONS ($\zeta = 0$, $\xi = 10.9\%$, LAG, FLAP)

FIGURE 8-6: GROUND RESONANCE MODE SHAPE ($\zeta = 0$, $\xi_R = 10.9\%$, LAG, FLAP)
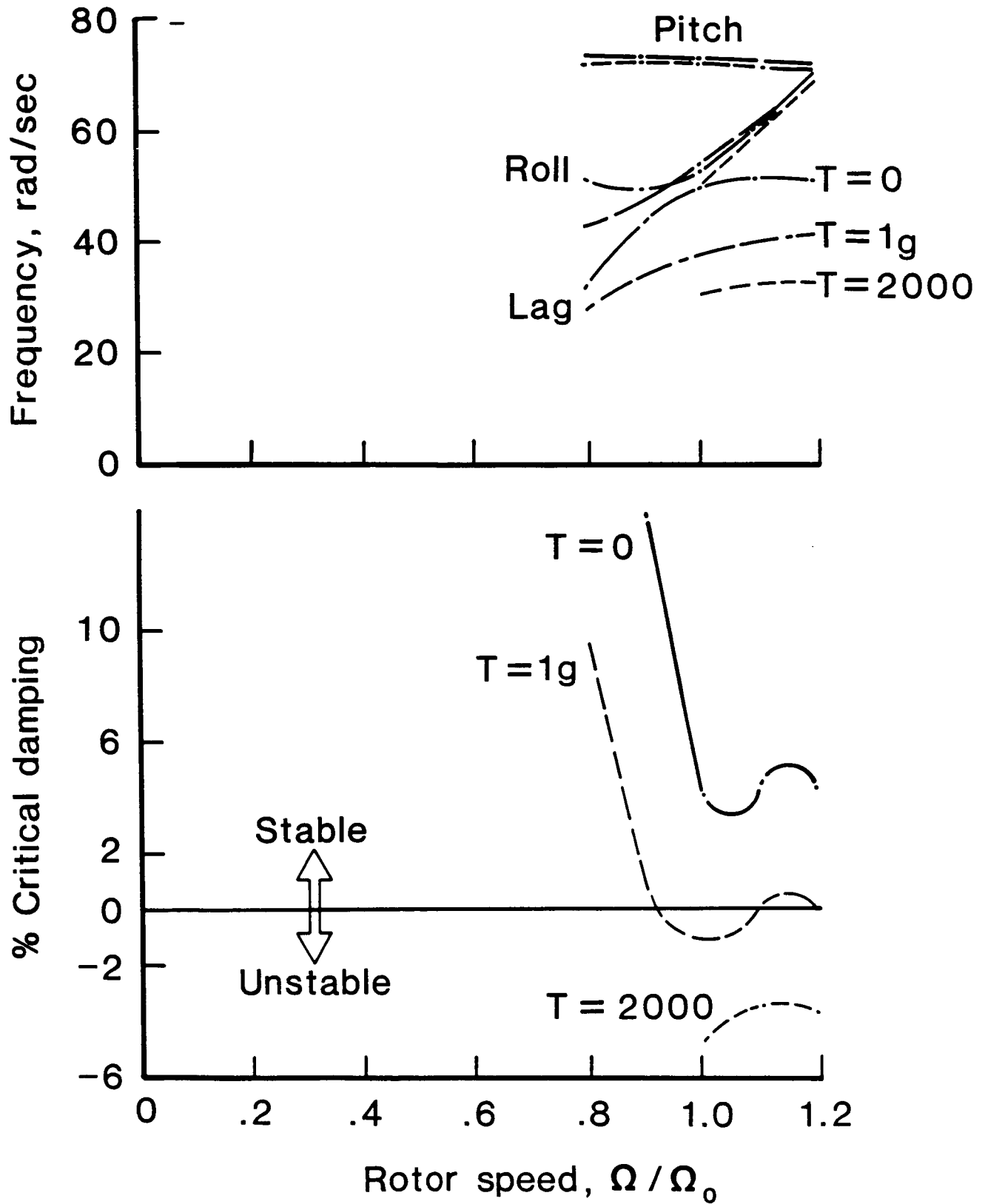
FIGURE 8-7: GROUND RESONANCE (ζ = AIR, ξ_R = 10.9%, LAG, FLAP, HUB ROTS.)
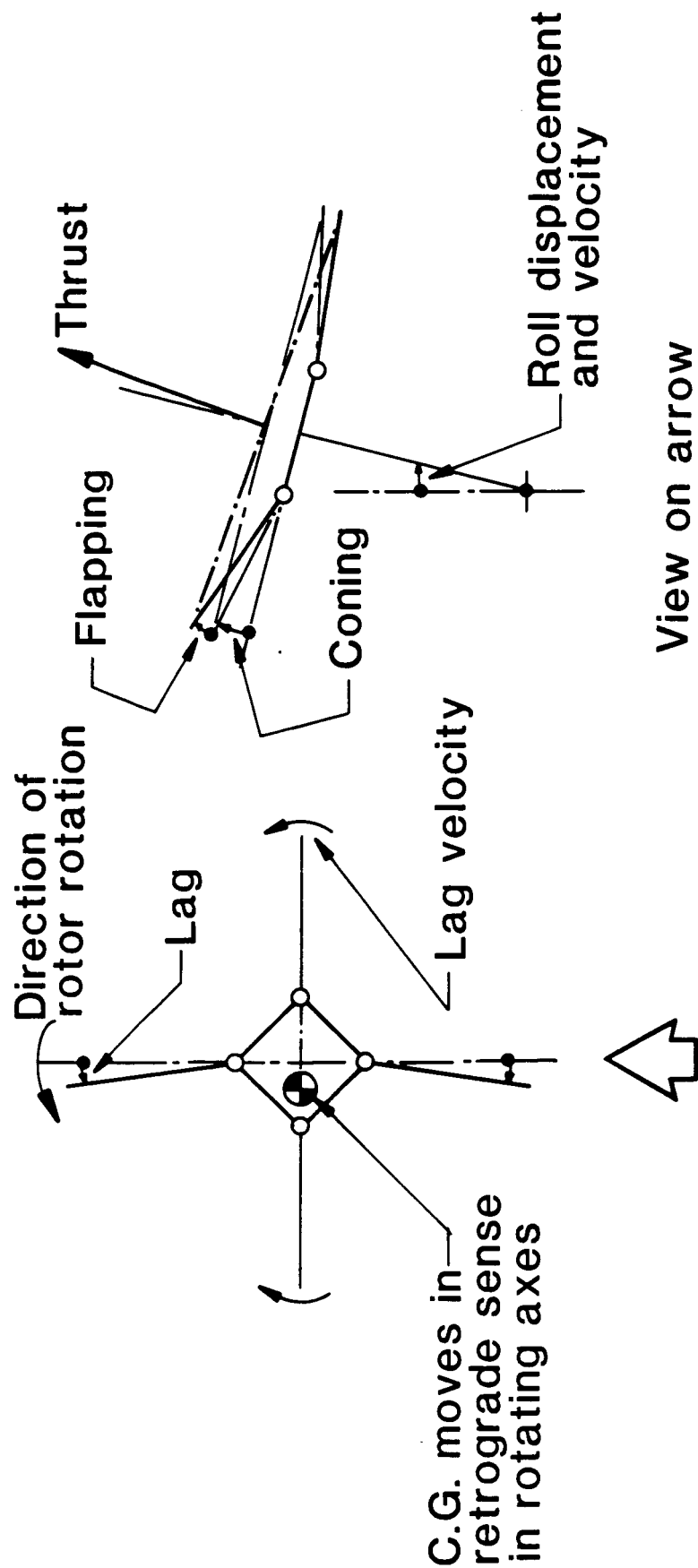
FIGURE 8-8: GROUND RESONANCE MODE SHAPE (δ = AIR, δ = 10.95, LAG, FLAP, HUB ROTS.) UNSTABLE MODE SHAPE SHOWS SOURCE OF NEGATIVE DAMPING FROM THRUST
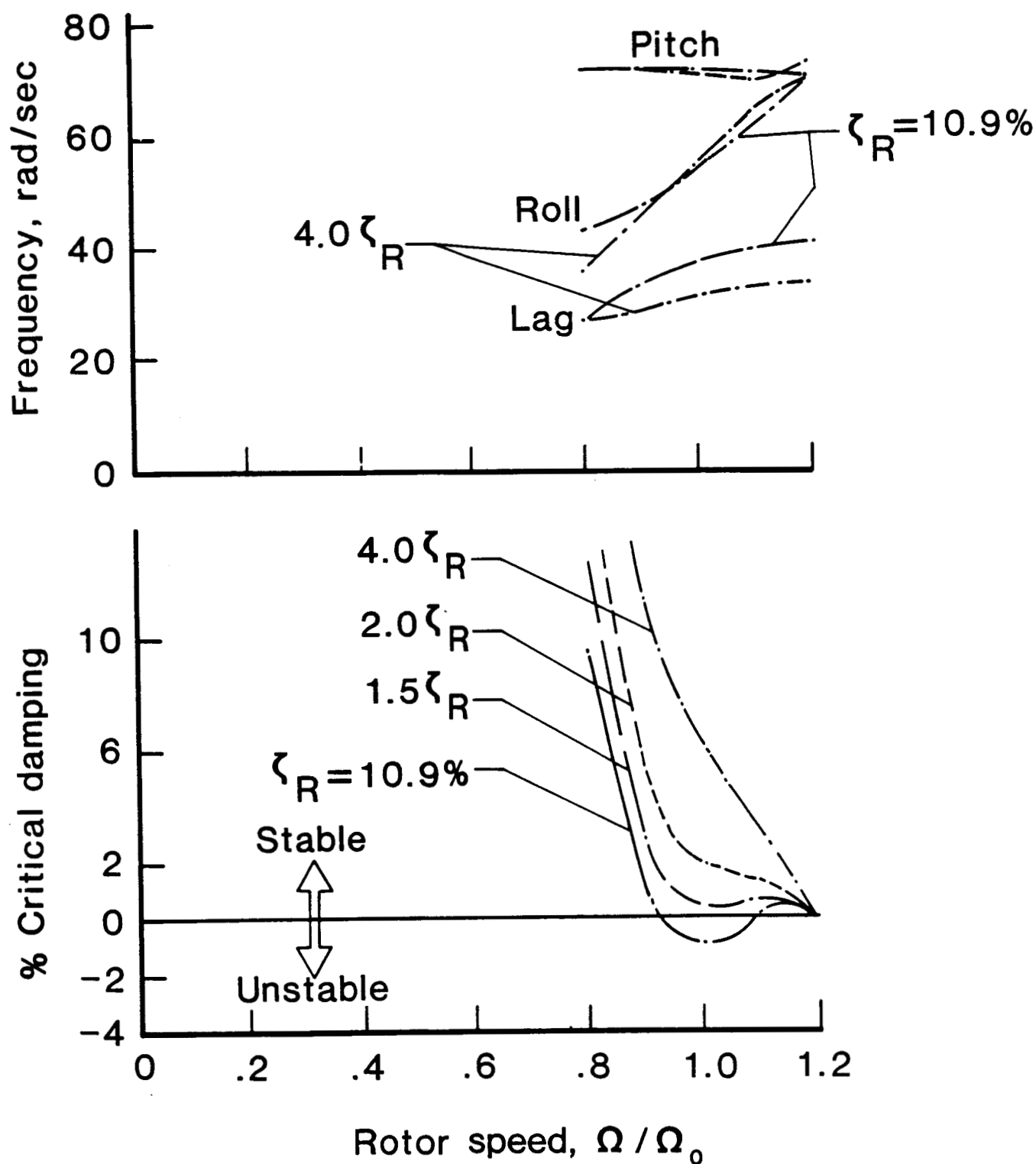
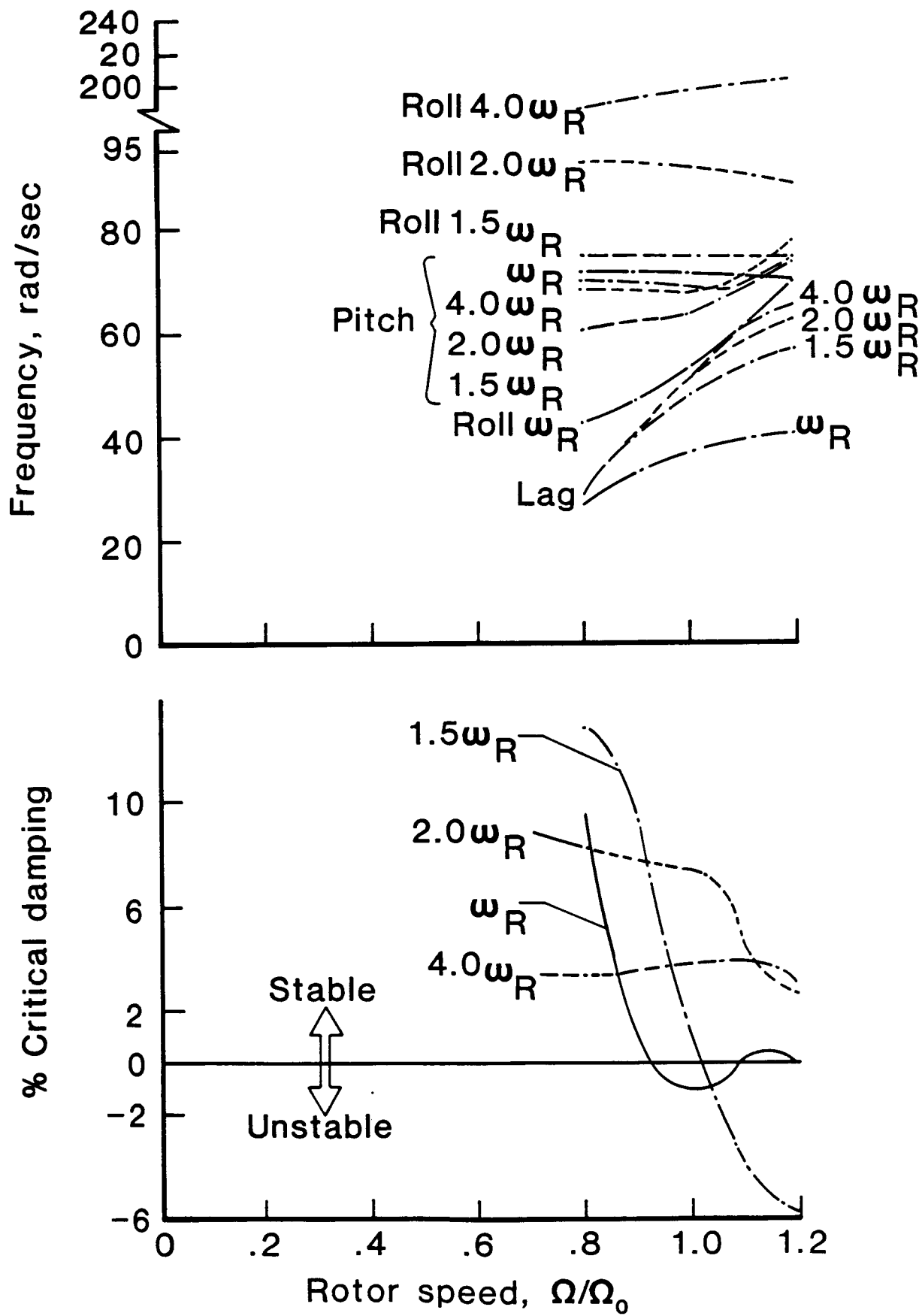FIGURE 8-9:   GROUND RESONANCE INCREASED BODY ROLL DAMPING (T = 1g, ξ_R = 10.9%, LAG, FLAP, HUB ROTS.)

FIGURE 8-10: GROUND RESONANCE INCREASED BODY ROLL FREQUENCY (T = 1g, ξ_R = 10.9%, LAG, FLAP, HUB ROTS.)
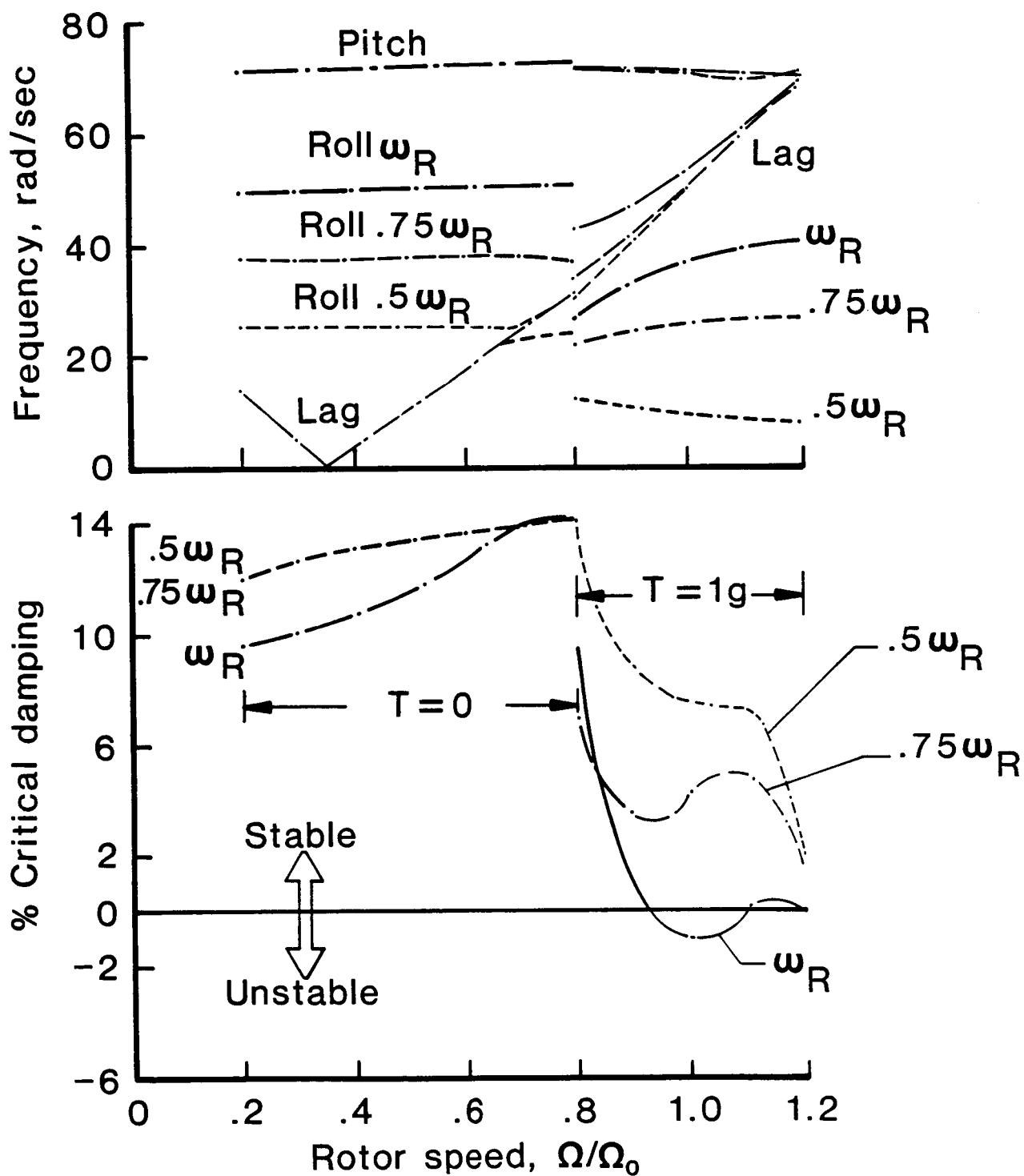
FIGURE 8-11: GROUND RESONANCE, ROTOR SPEED Ω/Ω_o DECREASED BODY ROLL FREQUENCY (ζ = AIR, ξ = 10.9%, LAG, FLAP, HUB ROTS.)

Table 2-1.

SCALE FACTORS FOR MACH SCALING IN AIR

Length	$S = 0.27$
Mach Number	1
Lock Number	1
Mass	S^3
Time	S
Force	S^2

Table 2-2.

AAH MAIN ROTOR PROPERTIES

	FULL SCALE	0.27 MODEL
Number of Blades	4	4
Blade Chord	21 in.	5.67 in.
Blade Tip Sweep	20^0	20^0
Blade Twist	-9^0	-9^0
Pitch Flap Coupling	0	0
Pitch Lag Coupling	0	0
Blade Radius	288 in.	77.76 in.
Blade Flap Hinge Offset	11 in.	2.97 in.
Blade Lag Hinge Offset	34.5 in.	9.32 in.
Normal Rotor Speed	289 rpm	1070.4 rpm

Table 2-3.

HUB DATA COMPARISON - 0.27 SCALE ROTOR

	Ideally Scaled	Actual
Hub Weight - lb.	3.29	6.55
Flapping Hardware		
Wt. - lb.	2.06	2.68
C.G. - In. from Centerline	6.95	6.66
I_θ - Lb.-In.^{2}	2.63	3.77
Strap Chordwise Stiffness - lb./in.	7695.	9157.
Control System Stiffness - $\frac{lb./in.}{rad.}$	6950.[1]	13,300.[2,3]

[1] Average value of longitudinal and lateral cyclic control system stiffness, see Reference 5.

[2] Total stiffness is composed of:

Pitch Link - lb./in.	4550
Pitch Housing - lb./in.	5800
GRMS Swashplate, Actuators, etc. - lb./in.	9820
(Pitch Link Offset = 2.565 in.)	

[3] The pitch links were deliberately fabricated to be stiffer than required, with the stipulation that wind tunnel personnel will measure the actual control stiffness and machine the pitch links to reduce their stiffness to the desired value.

Table 2-4.

BLADE DATA COMPARISON - 0.27 SCALE ROTOR

	Ideally Scaled	Actual	$\Delta\%$
c	5.67"	5.67"	.0
X_{EA}/c	20%		
EI_c	4.55×10^6 lb.-in.^{2}	4.44×10^6	-2.4
EI_f	109,500	106,950	-2.3
GJ	101,000	124,500	+23.2
m	.0368 lb/in.	.0368	.0
I_θ	.0684 lb-in.		
S_γ	101.3 lb-in.	107.5	+6.1
Removable Blade Wt.	3.04 lb.	3.24	+6.6
Blade Chordwise C.G./C	26.4%	26.5%	
Chordwise C.G. of Tip Section/C	25.8%	25.0%	
X_{FA}/c	27%	27%	
Airfoil	HH02/64A006	HH02/64A006	
X_{AC}/c	25.3 ÷ 28.2%	25.3 ÷ 28.2%	
θ_B	-9°	-9°	
Sweep	20° (from .93R to tip)	20°	

(note: X_{EA}/c through I_θ are bracketed as "in uniform blade section")

Table 2-5.

27% MACH SCALED DAMPER CHARACTERISTICS

to be Tested in the NASA Langley V/STOL Tunnel

A. Dynamic Characteristics at $73^\circ \pm 18^\circ$F

    1. Qualification Condition

        a. Preflex $\pm$ .054 in, 3 cycles

        b. Input - 0 $\pm$ .011 in at 535 CPM
           Spring rates after 1 minute

              $K' = 8100$ lb/in $\pm$ 15%
              $K'' = 5670$ lb/in $\pm$ 15%

        c. Input - 0 $\pm$ .054 in, at 535 CPM
           Spring rate at 5 seconds

              $K'' = 3240$ lb/in $\pm$ 15%

B. Fatigue Spectrum
   Design life of at least 200 hours

COND.	% OCCURRENCE	DEFLECTION (inches)
1	62.9388	.014 $\pm$ .007
2	24.5000	.014 $\pm$ .011
3	11.7000	.041 $\pm$ .019
4	.8200	.041 $\pm$ .030
5	.0270	.057 $\pm$ .041
6	.0124	.057 $\pm$ .051
7	.0018	.032 $\pm$ .068
8	1 per life	0 $\pm$ .141

C. Temperature Spectrum
   Ambient operating temperature range: 30°F to 120°F

TEMPERATURE, $^\circ$F	% OCCURRENCE
110	10%
75 $\pm$ 25°	80%
35	10%

Table 3-1.

MEASURED MODAL PROPERTIES OF THE GRMS

Mode Description	Gen. Model Mass lb-sec²/in.	Modal Frequency Hz	Modal Damping Percent CCR	Displacement Components at Hub				
				Longitudinal	Lateral	Vertical	Roll	Pitch
Sting Bending, Vertical	26.625	3.25	1.8	—	-.519	2.318	-.051	0.100
Gimbal Pitch	.402	12.0	13.7	—	0.092	-.344	0.004	0.074
Keel Pitch	2.111	16.0	2.7	—	-.013	-.210	0.009	0.028
Shaft Bending, Longitudinal	0.296	31.1	3.2	—	-.042	-.108	0.009	0.117
Sting Bending, Lateral	3.318	3.0	6.5	-.053	—	-.018	0.024	0.004
Motor Roll	0.106	8.9	5.4	-.086	—	.048	-.063	0.006
Keel Roll	0.680	16.4	3.0	-.029	—	.028	-.074	0.003
Keel-Motor Roll	0.386	26.2	10.8	-.632	—	.015	0.020	0.019
Shaft Bending, Lateral	0.435	43.7	8.3	-.480	—	.091	-.133	-.032
Shaft Bending, Lateral Motor Roll	0.396	57.0	4.5	-.350	—	0.107	-.249	-.027

⊕ Positive directions are: aft right up left nose up

Table 5-1.

GRMS FREQUENCIES WHEN COUPLED WITH ROTOR

GRMS MODES	----- COUPLED ROTOR/GRMS MODES - Hz -----			
	2% N_R	80% N_R	100% N_R	120% N_R
Roll - 8.9 Hz	8.13	7.6	7.73	7.86
Pitch - 12.0 Hz	11.45	11.3	11.3	11.2

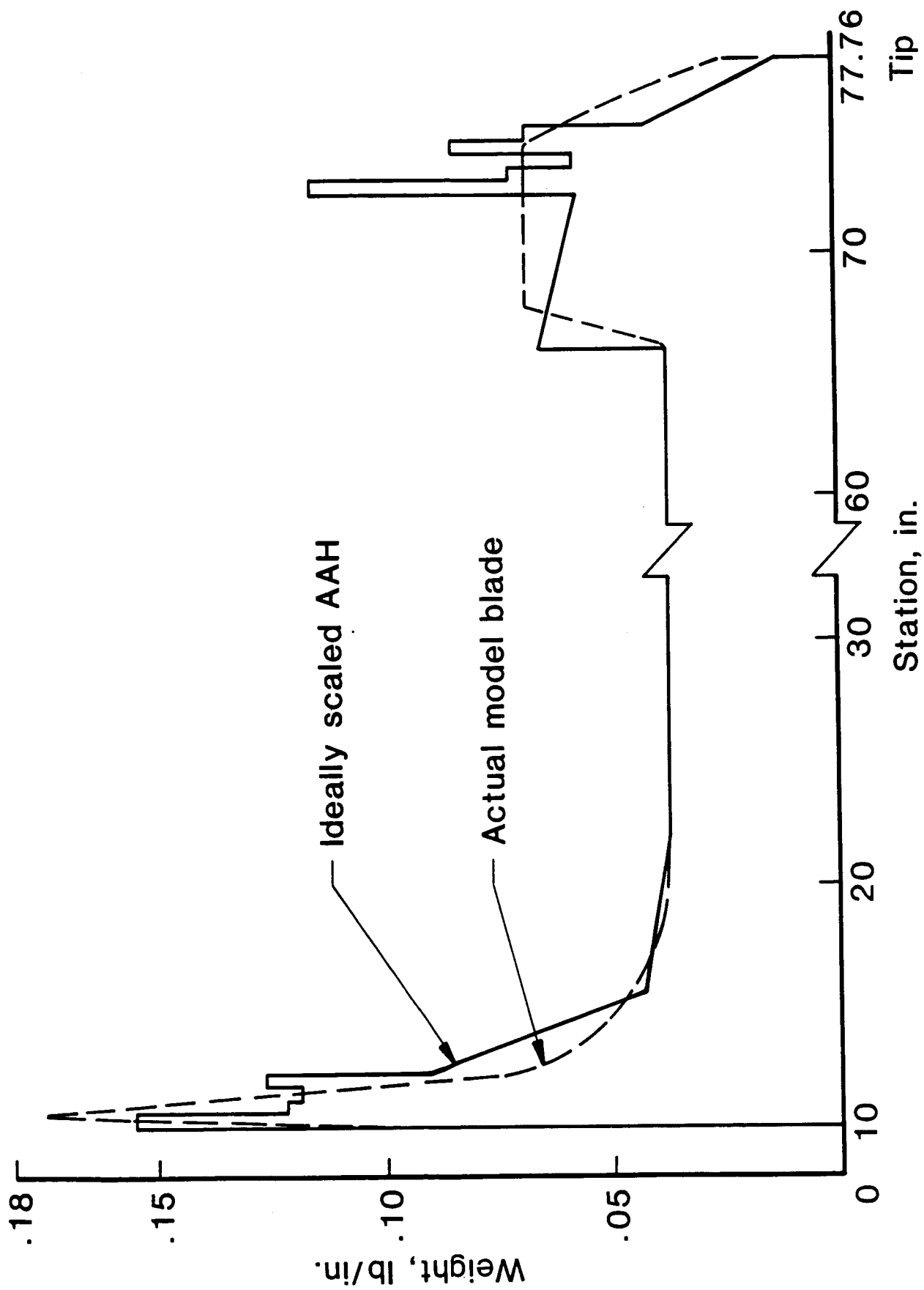APPENDIX A

. MODEL BLADE DATA
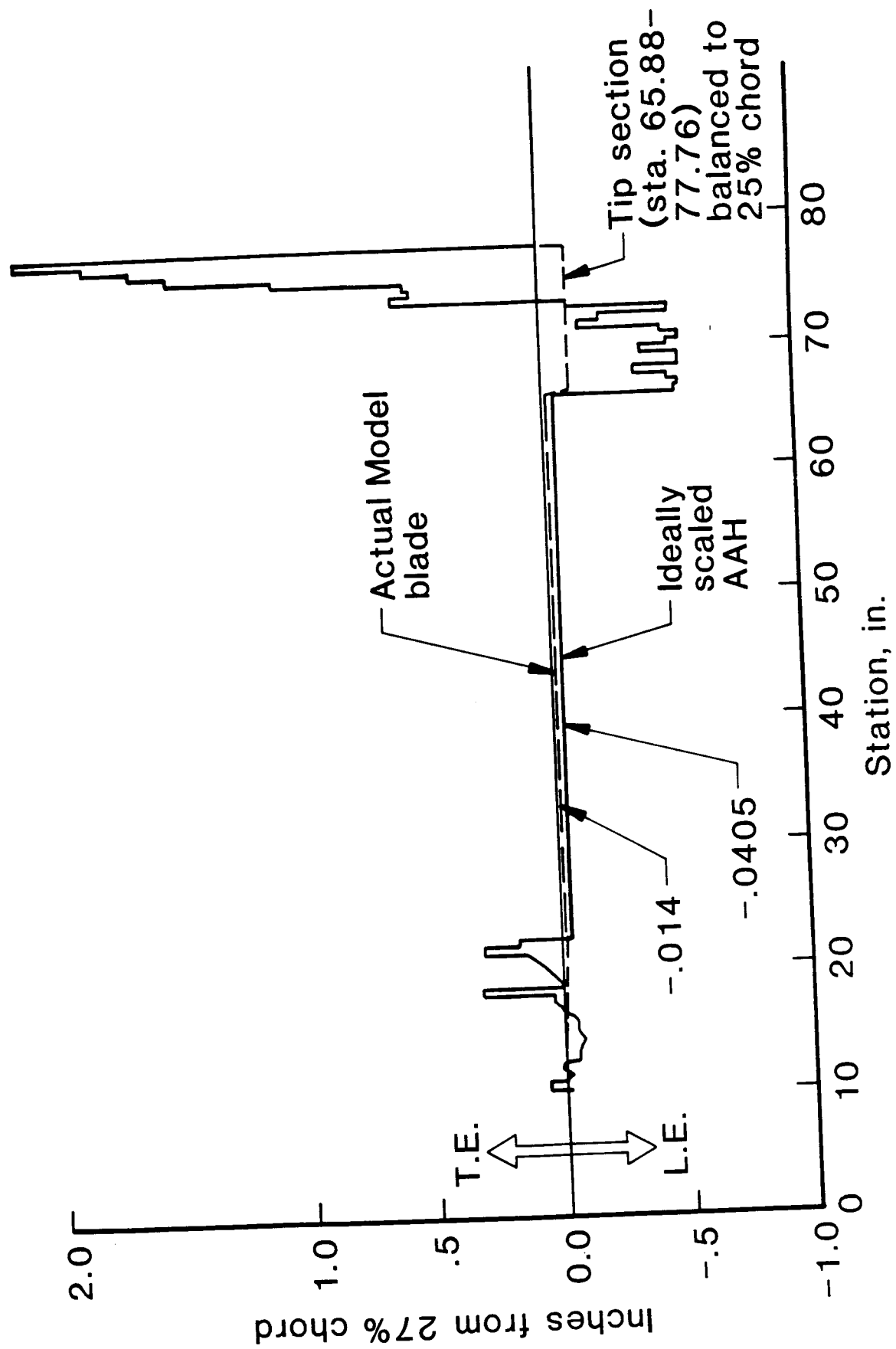
FIGURE A-1: .27 SCALE BLADE WT. DISTRIBUTION

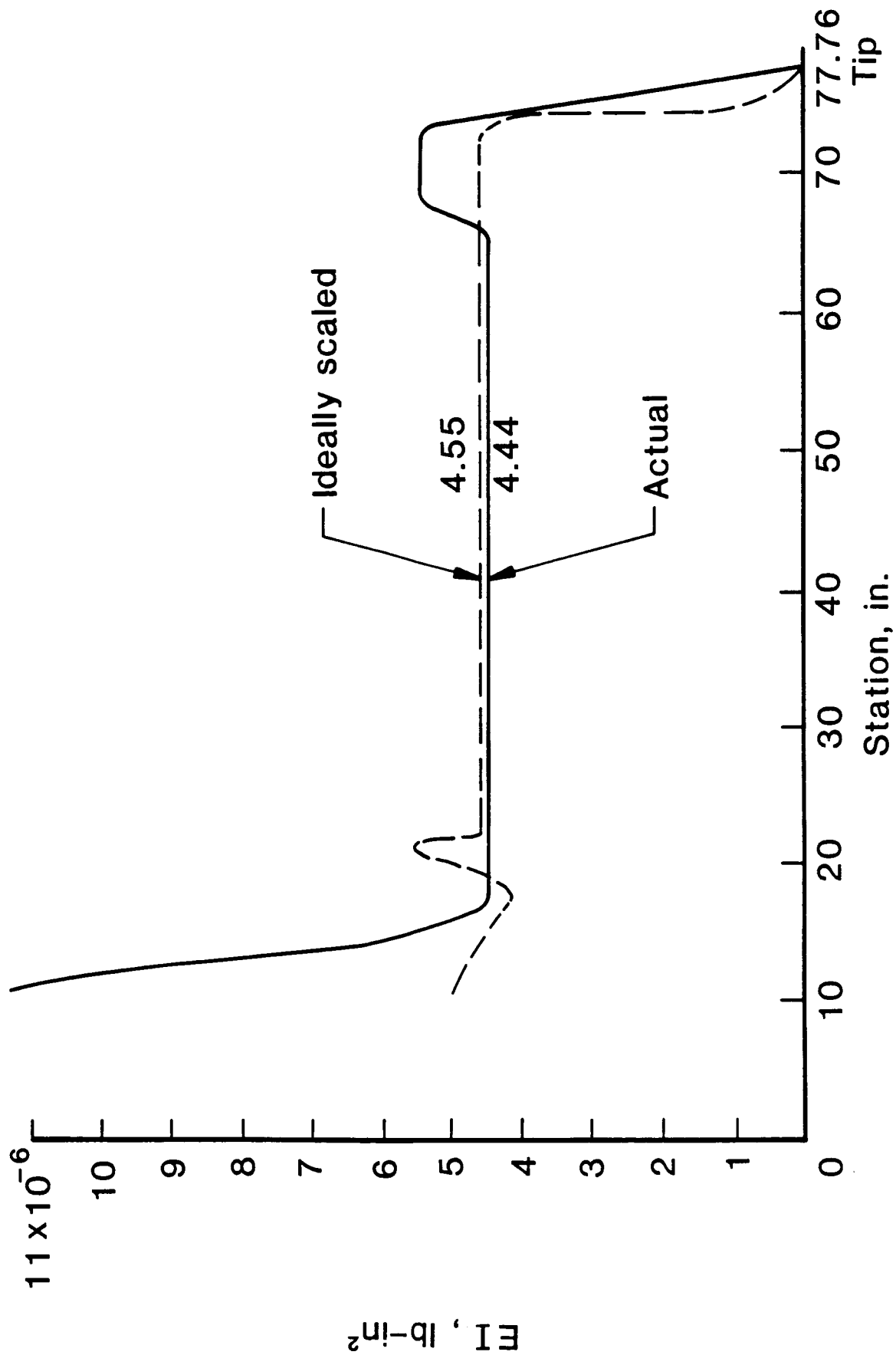FIGURE A-2: .27 SCALE BLADE CHORDWISE C.G. DISTRIBUTION

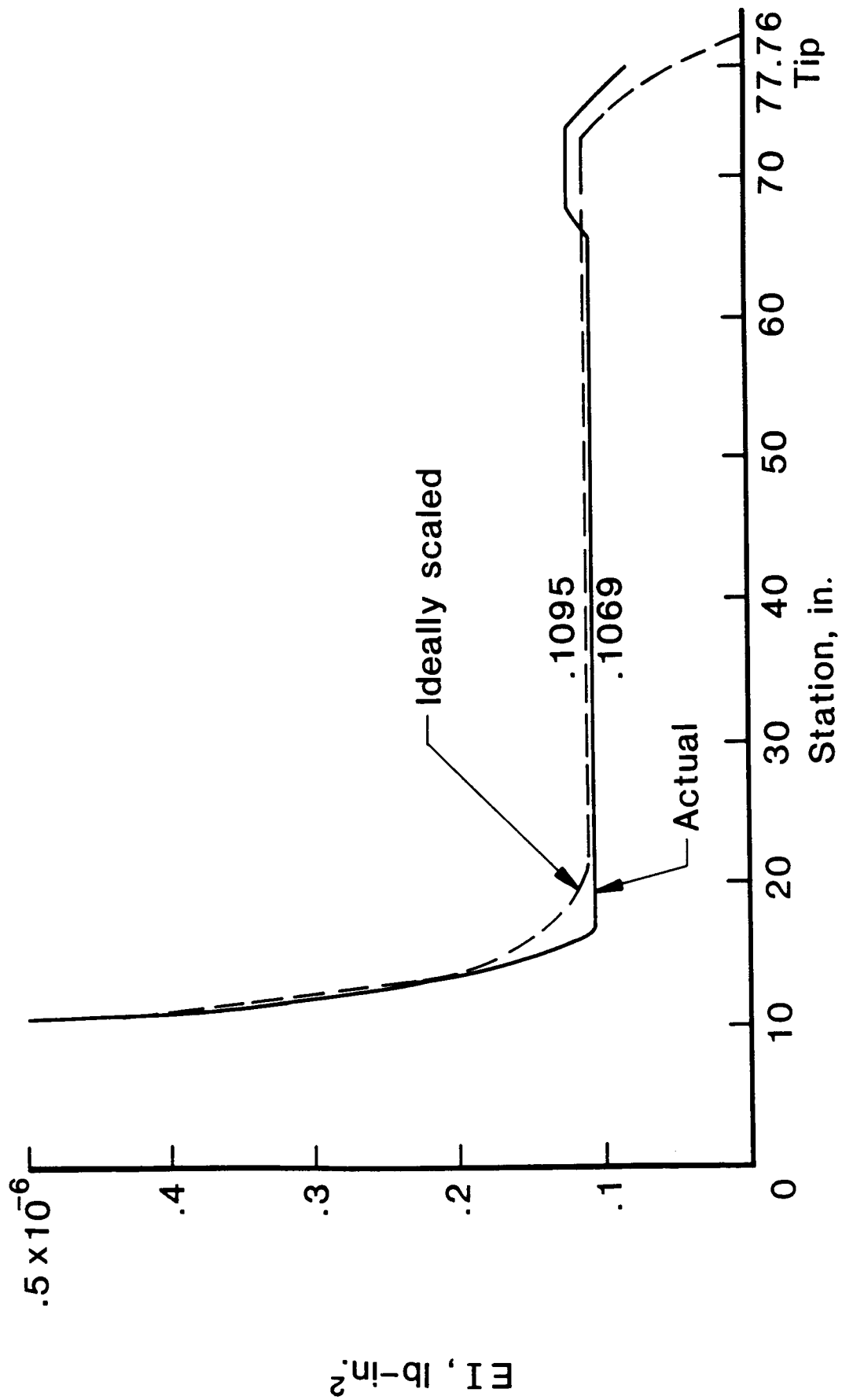FIGURE A-3: .27 SCALE BLADE IN-PLANE STIFFNESS DISTRIBUTION

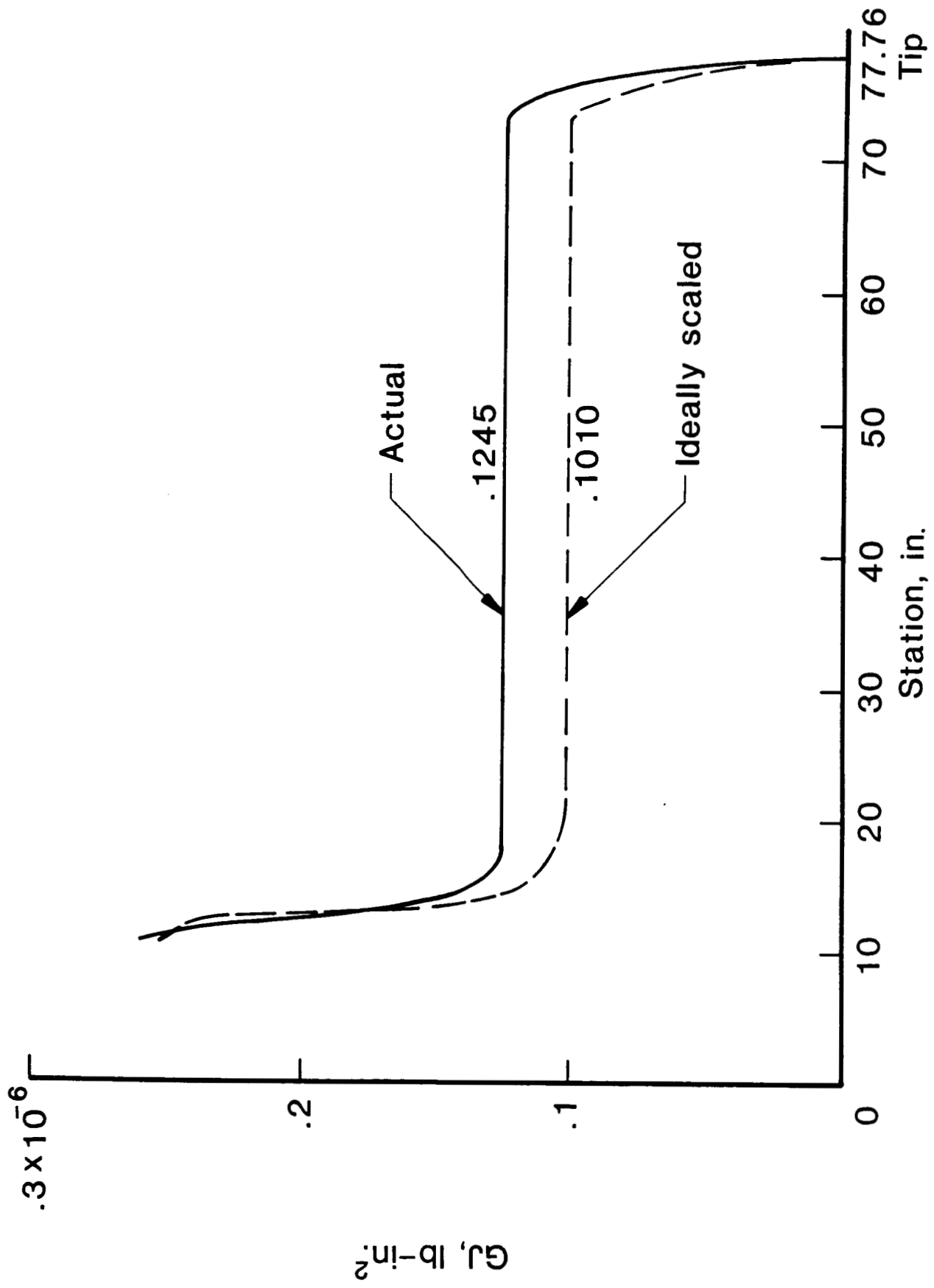FIGURE A-4: .27 SCALE BLADE FLAPPING STIFFNESS DISTRIBUTION

FIGURE A-5: .27 SCALE BLADE TORSIONAL STIFFNESS DISTRIBUTION

APPENDIX B

ADVANCED BLADE DYNAMICS

SUMMARY

NASA Langley is developing an advanced blade for the 0.27 Scale Model AAH rotor hub. An analysis was performed to evaluate its dynamic behavior. Figure 1 shows the resonance plot for the advanced blade compared with that of the ideally scaled (baseline) blade. The advanced blade, due to its different properties, see Table 1 and Figures 2 and 3, exhibits considerably different frequency placement. However, no critical resonances are predicted.

In addition, it should be pointed out that the deletion of the swept tip raises the distinct probability of reintroducing the problem of "Mach tuck" encountered by the Phase 1 AAH blades. HHI recommends that the advanced blade design be checked in that respect and in case a problem is predicted that a swept tip be incorporated. Adjustable tip weight similar to those in the baseline blade are mandatory for spanwise and chordwise balancing.

DISCUSSION

1.0 Blade Properties

A comparison of properties of the baseline vs. the advanced blade is shown in Table 1. Also, the blade planforms are shown in Figure 2 and blade weight distributions are compared in Figure 3. From this, it is seen that blade stiffnesses change by at most 15%. The advanced blade geometry, i.e., chord, planform, twist, cross-sectional offsets are considerably different. The blade distributed weight and total weight are very close to the baseline value. However, the first mass moment of inertia about the lag hinge, S_γ, is 30% lower. The reason for this is the difference in distributed weight in the tip section, see Figure 3. Apparently no tip weights are used in the advanced blade. The feathering inertia, I_θ, of the advanced blade is very large. Its value corresponds to a radius of gyration ($\zeta = \sqrt{I_\theta/m}$) of 29% chord which is about the same as that for a rectangular cross-section. In comparison, the baseline blade value is $\zeta = 24\%$ chord. The reason for this big difference is not apparent without having detailed information on the cross-section built up.

2.0 Frequency Placement

To better understand the changes in frequency placement seen in Figure 1, the advanced blade stiffness, geometry, and mass properties were added step by step to the baseline blade model. The resulting frequencies are shown in Table 2.

2.1 Stiffness

Adding the advanced blade stiffnesses to the baseline blade model increases the flap bending and torsional frequencies while lowering the chord bending frequency. These changes as well as their magnitudes are in accordance with the stiffness changes listed in Table 1.

2.2 Geometry

Adding the advanced blade geometry affects only the torsional modes. The elimination of sweep results in a reduced feathering inertia. This should raise the torsional frequencies, which is the case for the second torsion mode, but not the first torsion mode. This last fact is probably due to aerodynamic effects.

2.3 Mass

Lastly, the advanced blade mass properties are added and thus the complete advanced blade is modelled.

Inplane Modes: It is seen that the reduced mass in the tip area causes a considerable increase in the lag and chord bending frequencies ($\sim$ 16%).

Flapwise Modes: The reduced mass in the tip area will also contribute to an increase in flap bending frequencies. However its effect is opposed by the large weight of the blade root end fitting. The closer the blade root fitting is to antinode, the more it will contribute to lowering the frequency of a particular mode. Taking the amplitude at the blade root fitting divided by the tip amplitude as indication of relative motion, one obtains values of 0.38, 0.08, 0.09 for the first, second, and third flap bending modes. The change in frequencies for the corresponding modes is -9%, +13% and +2%. Thus it is seen that the large amplitude of the root end fitting in the case of the first flap bending mode (0.38) actually lowers the frequency of that mode. In general, Figure 1 shows that the low weight in the tip section reduces the amount of C.F.-stiffening for the flapwise modes. This manifests itself in the smaller increase of flap bending frequencies with RPM, as compared to the baseline blade.

Torsion Modes: As expected, the increase in feathering inertia causes a drop in frequency for both torsion modes.

CONCLUSIONS

The advanced blade is a dynamically different blade. However, Figure 1 shows no critical resonances.

RECOMMENDATIONS

The cross-sectional polar mass moment of inertia, I_θ, should be checked. Its value is unreasonably high.

Provisions for adjustable tip weights should be made to allow for spanwise and chordwise balancing of the blade. This would also be beneficial in making the advanced blade more dynamically similar to the baseline blade. In addition, the tip weights could be used to move the cross-sectional C.G. of the tip section further towards the leading edge. At the same time, the root end fitting should be lightened.

The advanced blade should be checked for the problem of "Mach tuck".
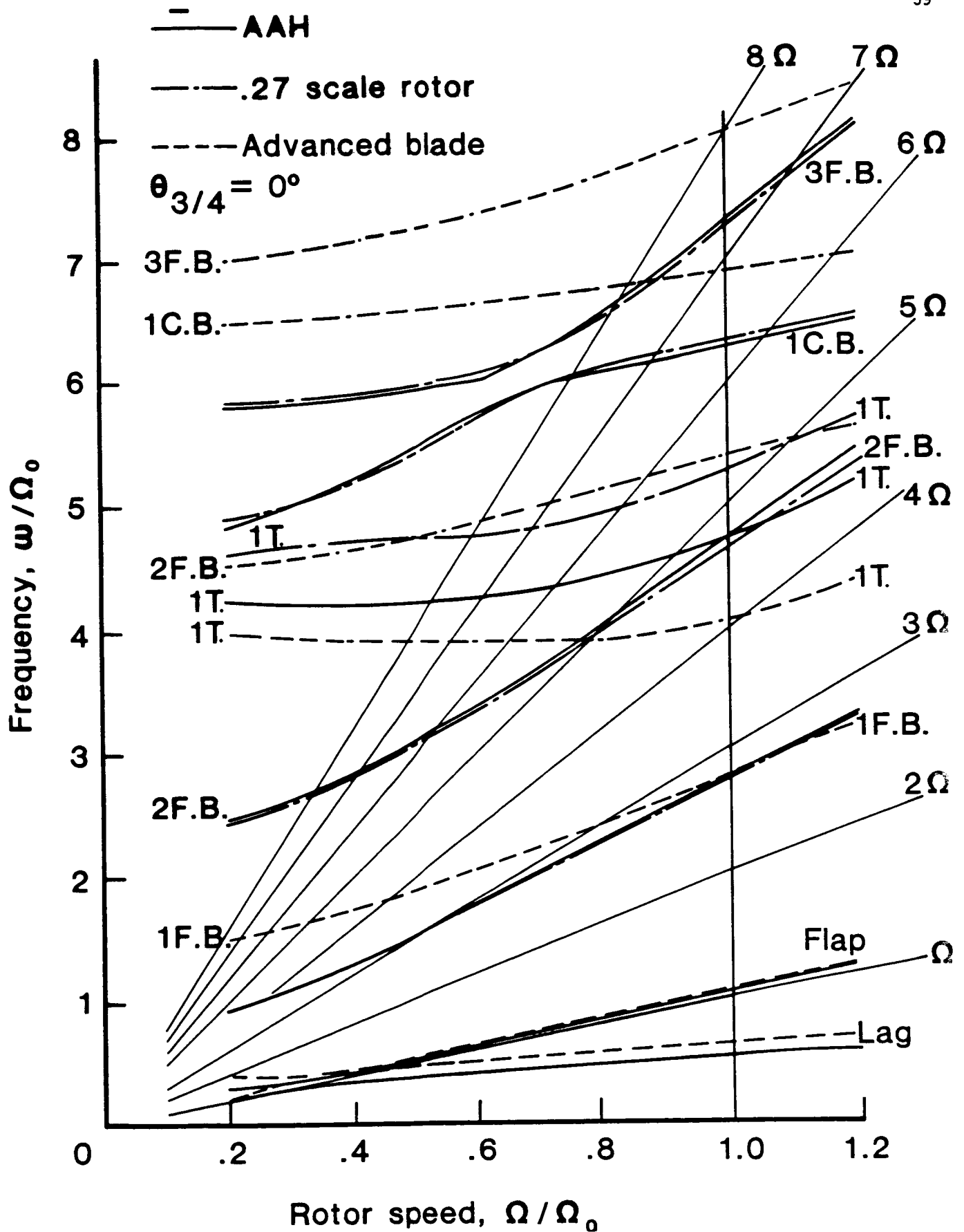
FKS/abw

Attachments

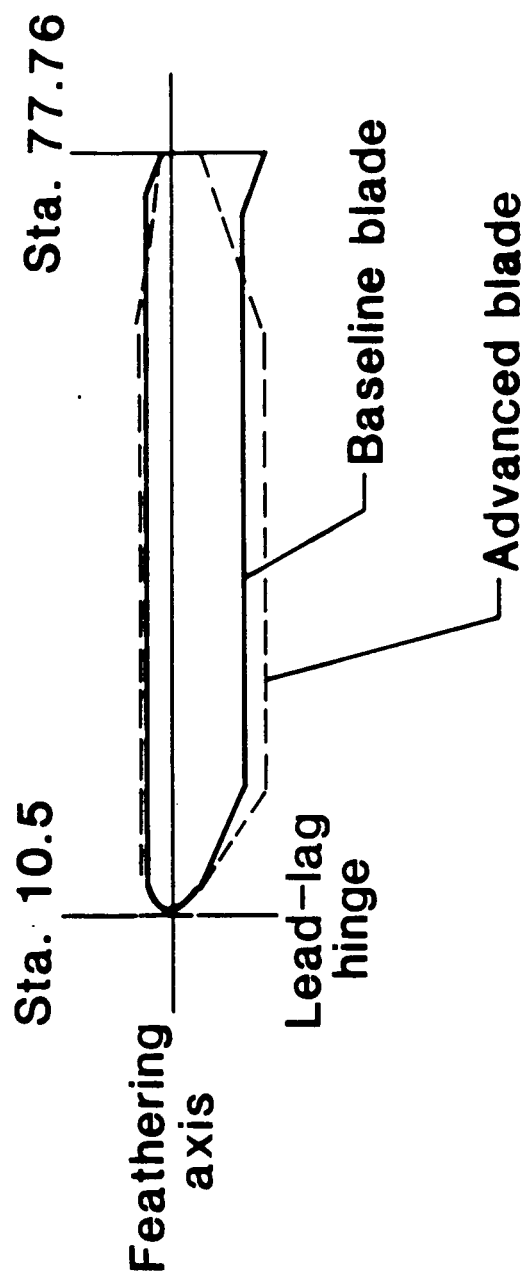FIGURE B-1: AAH M/R RESONANCE DIAGRAM ISOLATED BLADE
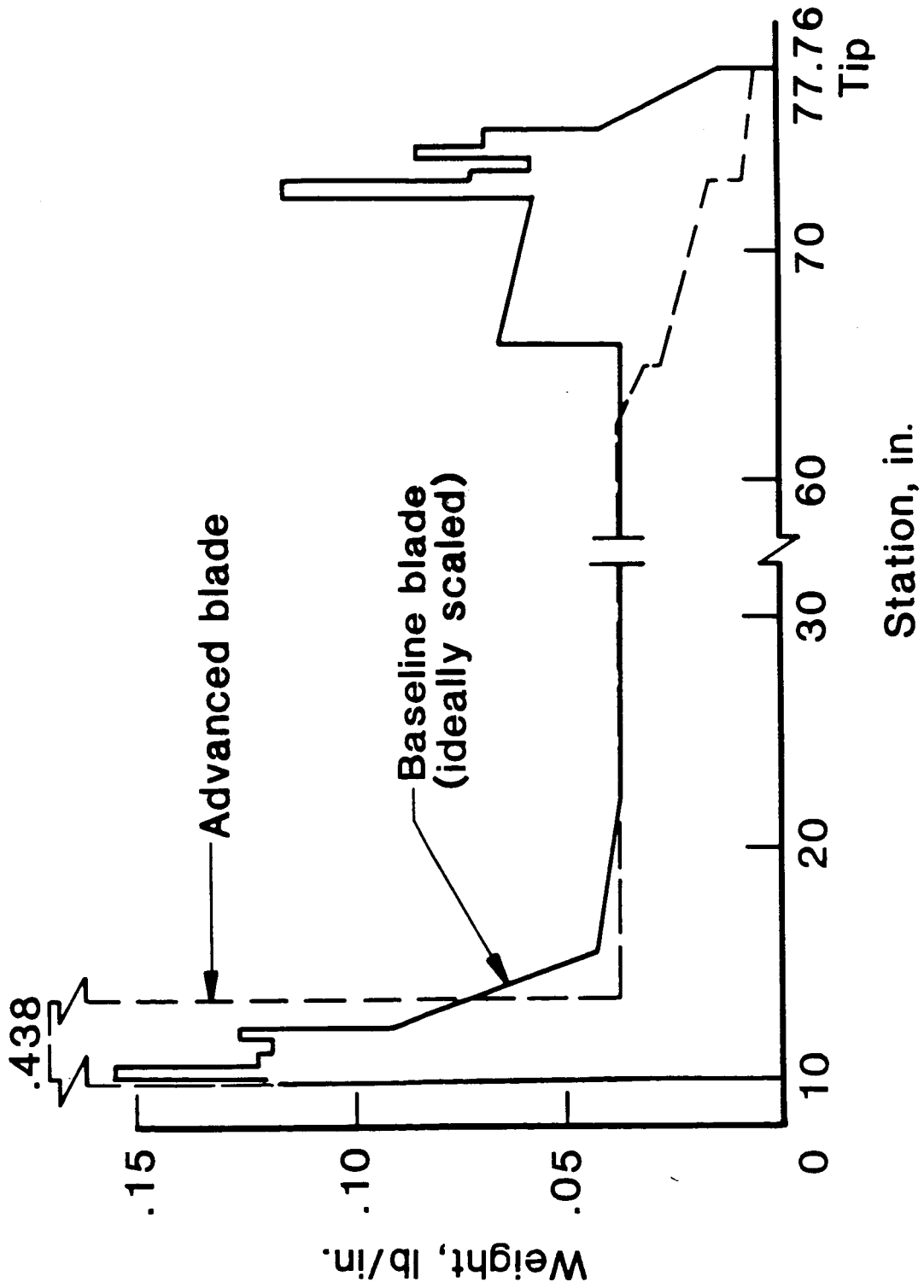
FIGURE B-2:   BLADE PLANFORM

FIGURE B-3: .27 SCALE ROTOR BLADE WEIGHT DISTRIBUTION

REPORT TITLE

REPORT NO.

PREPARED BY

CHECKED BY

MODEL NO.

SUBJECT

BLADE DATA COMPARISON — TABLE 1

	BASELINE (IDEALLY SCALED)	ADVANCED	Δ %
chord = c	5.67"	7"	+24%
x_{EA}/c	20%	26%	
EI_c	4.55×10^6 lb in^2	3.98×10^6	−13%
EI_f	109,500 lb in^2	124,200	+15%
GJ	101,000 lb in^2	116,500	+14%
m	.0368 lb/in	.0373	+1%
I_θ	.0684 lb-in	.1534	+124%
$S_g = \Sigma mr$	101.3 lb in	66.32 (w/o blade cuff)	−30%
REMOVABLE BLADE WT.	3.04 lb	3.29	+9%
BLADE CHORD-WISE C.G. /C	26.4%	26.2%	
x_{AC}/c	25.3 ÷ 28.2 %	25 ÷ 27%	
x_{FA}/c	27%	25%	
θ_B	−9°	−12°	
AIRFOIL	HH02	RC-10B3 B root RC-10B3 ↓ RC-08B3 tip	
TAPER	N/A	LINEAR from .81R to TIP $C_{TIP} = .35 C_{UNIFORM}$	
SWEEP	20° from .93R to TIP	N/A	

(IN UNIFORM BLADE SECTION)

FORM 9704 (REV 4/77)

Hughes Helicopters

SUBJECT
FREQUENCIES OF ISOLATED BLADE — TABLE B-2

COMPARISON OF BASELINE VS. ADVANCED BLADE FREQUENCIES ($^1/_{REV}$), $\Omega = \Omega_0$, $\theta_{3/4} = 0°$

	BASELINE BLADE (IDEALLY SCALED)	BASELINE BLADE w. ADV. BLADE STIFFNESS	BASELINE BLADE w. ADV. BLADE STIFFNESS & GEOMETRY	ADVANCED BLADE
LAG	.511	.511	.511	.608
FLAP	1.04	1.03	1.03	1.05
1 F.	2.75	3.03	3.02	2.78
1 T.	5.27	5.60	4.99	4.03
2 F.	4.62	4.84	4.74	5.39
1 C.	6.32	5.94	5.94	6.88
3 F.	7.25	7.98	7.83	8.03
2 T.	9.65	9.76	9.95	9.34

ORIGINAL PAGE IS
OF POOR QUALITY

FORM 9704 (REV 4/77)

Hughes Helicopters

1. Report No. NASA CR-178284	2. Government Accession No.	3. Recipient's Catalog No.
4. Title and Subtitle Aeroelasticity and Mechanical Stability Report, 0.27 Mach Scale Model of the YAH-64 Advanced Attack Helicopter		5. Report Date May 1987
		6. Performing Organization Code
7. Author(s) F.K. Straub and R.A. Johnston		8. Performing Organization Report No. 150-V-1003
9. Performing Organization Name and Address McDonnell Douglas Helicopter Company 5000 East McDowell Road Mesa, AZ 85205-9797		10. Work Unit No. 505-61-51-10
		11. Contract or Grant No. NAS1-16475
12. Sponsoring Agency Name and Address National Aeronautics and Space Administration Washington, D.C. 20546		13. Type of Report and Period Covered Contractor Report
		14. Sponsoring Agency Code

15. Supplementary Notes

Langley Technical Monitor: Henry L. Kelley

Final Report

16. Abstract

A 27% dynamically scaled model of the AH-64 Advanced Attack Helicopter main rotor and hub has been designed and fabricated. The model will be tested in the NASA Langley Research Center V/STOL wind tunnel using the General Rotor Model System (GRMS).

This report documents the studies performed to ensure dynamic similarity of the model with its full scale parent. It also contains a preliminary aeroelastic and aeromechanical substantiation for the rotor installation in the wind tunnel. From the limited studies performed no aeroelastic stability or load problems are projected. To alleviate a projected ground resonance problem, a modification of the roll characteristics of the GRMS is recommended.

17. Key Words (Suggested by Authors(s)) Model Helicopter Rotor, Aeroelasticity, Aeromechanical Stability	18. Distribution Statement Unclassified - Unlimited Subject Category 02		
19. Security Classif.(of this report) Unclassified	20. Security Classif.(of this page) Unclassified	21. No. of Pages 67	22. Price A04